

This discussion paper is/has been under review for the journal Atmospheric Chemistry and Physics (ACP). Please refer to the corresponding final paper in ACP if available.

LIVAS: a 3-D multi-wavelength aerosol/cloud climatology based on CALIPSO and EARLINET

V. Amiridis¹, E. Marinou¹, A. Tsekeli¹, U. Wandinger², A. Schwarz²,
E. Giannakaki³, R. Mamouri⁴, P. Kokkalis¹, I. Binietoglou⁵, S. Solomos¹,
T. Herekakis¹, S. Kazadzis⁶, E. Gerasopoulos⁶, D. Balis⁷, A. Papayannis⁸,
C. Kontoes¹, K. Kourtidis⁹, N. Papagiannopoulos¹⁰, L. Mona¹⁰, G. Pappalardo¹⁰,
O. Le Rille¹¹, and A. Ansmann²

¹Institute for Astronomy, Astrophysics, Space Applications and Remote Sensing,
National Observatory of Athens, Athens, 15236, Greece

²Leibniz Institute for Tropospheric Research (TROPOS), Leipzig, Germany

³Finnish Meteorological Institute, Kuopio Unit, Finland

⁴Cyprus University of Technology, Limassol, Cyprus

⁵National Institute of R&D for Optoelectronics, Bucharest, Romania

⁶Institute of Environmental Research and Sustainable Development,
National Observatory of Athens, Athen, Greece

⁷Aristotle University of Thessaloniki, Thessaloniki, Greece

⁸National Technical University of Athens, Zografou, Greece

ACPD

15, 2247–2304, 2015

LIVAS: a 3-D
multi-wavelength
aerosol/cloud
climatology

V. Amiridis et al.

Title Page

Abstract

Introduction

Conclusions

References

Tables

Figures

◀

▶

◀

▶

Back

Close

Full Screen / Esc

Printer-friendly Version

Interactive Discussion



⁹School of Engineering, Democritus University of Thrace, Xanthi, Greece

¹⁰Istituto di Metodologie per l'Analisi Ambientale, Consiglio Nazionale delle Ricerche, Potenza, Italy

¹¹European Space Agency, European Space Research and Technology Center, Noordwijk, the Netherlands

Received: 18 December 2014 – Accepted: 13 January 2015 – Published: 23 January 2015

Correspondence to: V. Amiridis (vamoir@noa.gr)

Published by Copernicus Publications on behalf of the European Geosciences Union.

ACPD

15, 2247–2304, 2015

LIVAS: a 3-D
multi-wavelength
aerosol/cloud
climatology

V. Amiridis et al.

Title Page

Abstract

Introduction

Conclusions

References

Tables

Figures



Back

Close

Full Screen / Esc

Printer-friendly Version

Interactive Discussion



Abstract

We present LIVAS, a 3-dimensional multi-wavelength global aerosol and cloud optical climatology, optimized to be used for future space-based lidar end-to-end simulations of realistic atmospheric scenarios as well as retrieval algorithm testing activities. LIVAS database provides averaged profiles of aerosol optical properties for the potential space-borne laser operating wavelengths of 355, 532, 1064, 1570 and 2050 nm and of cloud optical properties at the wavelength of 532 nm. The global climatology is based on CALIPSO observations at 532 and 1064 nm and on aerosol-type-dependent spectral conversion factors for backscatter and extinction, derived from EARLINET ground-based measurements for the UV and scattering calculations for the IR wavelengths, using a combination of input data from AERONET, suitable aerosol models and recent literature. The required spectral conversion factors are calculated for each of the CALIPSO aerosol types and are applied to CALIPSO extinction and backscatter data correspondingly to the aerosol type retrieved by the CALIPSO aerosol classification scheme. A cloud climatology based on CALIPSO measurements at 532 nm is also provided, neglecting wavelength conversion due to approximately neutral scattering behavior of clouds along the spectral range of LIVAS. Averages of particle linear depolarization ratio profiles at 532 nm are provided as well. Finally, vertical distributions for a set of selected scenes of specific atmospheric phenomena (e.g., dust outbreaks, volcanic eruptions, wild fires, polar stratospheric clouds) are analyzed and spectrally converted so as to be used as case studies for space-borne lidar performance assessments. The final global climatology includes 4-year (1 January 2008–31 December 2011) time-averaged CALIPSO data on a uniform grid of 1×1 degree with the original high vertical resolution of CALIPSO in order to ensure realistic simulations of the atmospheric variability in lidar end-to-end simulations.

ACPD

15, 2247–2304, 2015

Discussion Paper | Discussion Paper

LIVAS: a 3-D multi-wavelength aerosol/cloud climatology

V. Amiridis et al.

[Title Page](#)

[Abstract](#)

[Introduction](#)

[Conclusions](#)

[References](#)

[Tables](#)

[Figures](#)

◀

▶

◀
Back

▶
Close

[Full Screen / Esc](#)

[Printer-friendly Version](#)

[Interactive Discussion](#)



1 Introduction

A general methodology to test the ability of candidate future space-borne remote-sensing instruments to observe atmospheric quantities is the application of their processing algorithms on simulated datasets. The datasets are usually based on the instrument characteristics and a description of the atmospheric state. Especially for active remote sensors as lidars, the vertical dimension should be included in the simulations. Global distributions of such data are available today due to the launch of the Cloud-Aerosol Lidar with Orthogonal Polarization (CALIOP) instrument on board the Cloud-Aerosol Lidar and Infrared Pathfinder Satellite Observations (CALIPSO) mission of NASA/CNES in June 2006 (Winker et al., 2009). Ever since, CALIPSO provides global aerosol and cloud vertical distributions to the scientific community through analysis of CALIOP backscatter observations at the operating wavelengths of 532 and 1064 nm.

The technique of active remote sensing of the atmosphere by lidar has been also chosen for two of the future ESA Earth Explorer Missions, namely the Atmospheric Dynamics Mission Aeolus (ADM-Aeolus; Stoffelen et al., 2005) and the Earth Clouds, Aerosols and Radiation Explorer (EarthCARE, ESA-SP-1279(1); Illingworth et al., 2014), and was further proposed for the Advanced Space Carbon and Climate Observation of Planet Earth (A-SCOPE), one of the candidates for the 7th Earth Explorer mission. Atmospheric Laser Doppler Instrument (ALADIN) on-board ADM-Aeolus and ATmospheric LIDar (ATLID) on-board EarthCARE are two High Spectral Resolution Lidars (HSRLs) operating at 355 nm and detecting the backscatter signal from atmospheric aerosols, clouds and molecules in order to retrieve the horizontal component of the wind vector with Doppler techniques (ALADIN) and the vertical profiles of aerosol and cloud backscatter, extinction and particle depolarization (ATLID). The instrument design proposed for the A-SCOPE mission is an Integrated Path Differential Absorption (IPDA) lidar, aiming at measuring column-averaged dry-air CO₂ mixing ratios with high

[Title Page](#)[Abstract](#)[Introduction](#)[Conclusions](#)[References](#)[Tables](#)[Figures](#)[◀](#)[▶](#)[Back](#)[Close](#)[Full Screen / Esc](#)[Printer-friendly Version](#)[Interactive Discussion](#)

Due to its spatial restrictions, the current ESA RMA is not representative for global simulations. The correct performance assessment of current and future ESA lidar instruments requires the development of a refined aerosol and cloud optical database with high spatial resolution for the Planetary Boundary Layer (PBL), the free troposphere (FT) and the stratosphere. An appropriate RMA should be representative of both statistical atmospheric information (i.e. per atmospheric region, climate zone and season) and deterministic information (i.e. extended atmospheric scenes with, e.g., Saharan dust events, biomass-burning aerosol events, volcanic eruption events, polar stratospheric cloud events, convective cloud events). Moreover, the RMA should include multi-wavelength parameters so as to cover the spectral domain of future HSRL and IPDA lidar missions, specifically the three harmonic operating wavelengths of Nd:YAG lasers (355, 532 and 1064 nm) and typical wavelengths of future IPDA lidars in the SWIR spectral domain (1.57 and 2.05 μm).

Over the recent years, the European Aerosol Research Lidar Network (EARLINET, <http://www.earlinet.org/>; Pappalardo et al., 2014) and the Aerosol Robotic Network (AERONET, <http://aeronet.gsfc.nasa.gov/>; Holben et al., 1998) ground-based lidar and sunphotometer networks, respectively, along with the CALIPSO backscatter lidar mission have provided new resources that can be used for the elaboration of such a multi-wavelength database for typical laser operating wavelengths. Additionally, several air-

LIVAS: a 3-D multi-wavelength aerosol/cloud climatology

V. Amiridis et al.

Title Page

Abstract

Introduction

Conclusions

References

Tables

Figures

Tables

Figures

1

1

Back

Close

Full Screen / Esc

[Printer-friendly Version](#)

Interactive Discussion



borne and ground-based field experiments involving in-situ instrumentation together with HSRL and multi-wavelength Raman lidar systems have been performed over the last twenty years and can be very useful for the consolidation of such a RMA.

In this paper we present the “Lidar climatology of Vertical Aerosol Structure for space-based lidar simulation studies” (LIVAS) which is a RMA aiming to provide profiles of aerosol and cloud optical properties on a global scale, that can be used for the simulation of realistic atmospheric scenarios in current and future lidar end-to-end simulations and retrieval algorithm testing activities. For HSRL and IPDA lidar applications, LIVAS addresses the wavelength dependency of aerosol optical properties for the following laser operating wavelengths: 355, 532, 1064 nm, 1.57 and 2.05 μm . Moreover, LIVAS includes regional and seasonal statistics of aerosol and cloud extensive and intensive optical properties in terms of backscatter coefficient, extinction coefficient and particle linear depolarization ratio. Furthermore, vertical profiles of extensive and intensive optical properties referring to specific atmospheric scenes for a set of selected scenarios are provided (i.e. Saharan dust, smoke from biomass burning, ash from volcano eruptions, polar stratospheric clouds). The data used for the development of LIVAS are presented in Sect. 2 while the methodologies followed are given in Sect. 3. LIVAS product and its validation are presented in Sect. 4, and the paper closes with our conclusions in Sect. 5.

20 2 Data

2.1 The CALIPSO Level 2 product

CALIOP, the principal instrument on board the CALIPSO satellite, part of the NASA A-Train, is a standard dual-wavelength (532 and 1064 nm) backscatter lidar, operating a polarization channel at 532 nm (Winker et al., 2009). CALIOP has been acquiring high-resolution profiles of the attenuated backscatter of aerosols and clouds at 532 and 1064 nm along with polarized backscatter in the visible channel since 2006 (Winker et

Title Page	
Abstract	Introduction
Conclusions	References
Tables	Figures
	
	
Back	Close
Full Screen / Esc	
Printer-friendly Version	
Interactive Discussion	



al., 2009). The horizontal resolution of CALIPSO is 1/3 km while the vertical resolution is 60 m in the tropospheric region (between the surface and 20 km) and 180 m in the stratospheric region (between 20 and 30 km). This data is distributed as part of CALIPSO Level 1 products.

After calibration and range correction, cloud and aerosol layers are identified and aerosol backscatter and extinction at 532 and 1064 nm are retrieved as part of the Level 2 product. The product is produced by the application of a succession of algorithms that are described in detail in a special issue of the Journal of Atmospheric and Oceanic Technology (e.g., Winker et al., 2009). In brief, the CALIOP Level 2 retrieval scheme is composed of feature detection and subtyping algorithms (modules that classify features according to layer type and sub-type), and an extinction retrieval algorithm that estimates the aerosol backscatter and extinction coefficient profile and total column aerosol optical depth (AOD) using an assumed lidar ratio (LR) for each detected aerosol layer. The final CALIPSO Level 2 product includes the vertical location of layers (Vaughan et al., 2009), the discrimination of aerosol layers from clouds (Liu et al., 2009), the categorization of the aerosol layers in six subtypes (dust, marine, smoke, polluted dust, polluted continental, and clean continental; Omar et al., 2009), and AOD estimations for each layer detected (Young and Vaughan, 2009). Due to CALIOP's sensitivity to polarization at 532 nm, the depolarization arising from scattering from non-spherical dust particles serves as an independent means of discrimination between dust and other aerosol species. In this study we use the Version 3 of the Level 2 product (Young and Vaughan, 2009).

2.2 The EARLINET product

EARLINET (<http://www.earlinet.org>) has been operating since 2000 aiming to establish a quantitative and comprehensive database for the aerosol vertical, spatial and temporal distribution of aerosols on the European continental scale (Pappalardo et al., 2014). To date, EARLINET includes 27 stations in 16 countries performing lidar observations on a regular schedule of one daytime measurement per week around noon

Title Page

Abstract

Introduction

Conclusions

References

Tables

Figures

◀

▶

◀

▶

Back

Close

Full Screen / Esc

Printer-friendly Version

Interactive Discussion



and two nighttime measurements per week with low background light in order to perform Raman extinction measurements. The first volumes of the EARLINET database have been published in biannual volumes at the World Data Center for Climate (The EARLINET publishing group 2000–2010, 2014a, b). In addition to the routine measurements, further observations are devoted to monitor special events such as Saharan dust outbreaks, forest fires and volcano eruptions (The EARLINET publishing group 2000–2010, 2014d, e). Moreover, since 14 June 2006 EARLINET has carried out collocated measurements with CALIPSO during nearby overpasses, following a strategy defined on the basis of the ground-track data analysis provided by NASA (Pappalardo et al., 2010; The EARLINET publishing group 2000–2010, 2014c).

EARLINET operation is coordinated such as to ensure instrument standardization and consistent retrievals within the network. This harmonization is achieved through the application of a rigorous quality-assurance program addressing both instrument performance (Matthias et al., 2004; Freudenthaler et al., 2010) and evaluation of the algorithms (Böckmann et al., 2004; Pappalardo et al., 2004).

The 14-year EARLINET database contains a large data set of the aerosol lidar ratio retrieved from simultaneous and independent lidar measurements of aerosol extinction and backscatter coefficients. Moreover, this multi-wavelength database facilitates the retrieval of extinction and backscatter spectral dependence for different aerosol types after a proper layer identification and characterization. Such intensive properties are of fundamental importance for the estimation of aerosol extinction from pure backscatter lidar measurements such as conducted by CALIPSO (i.e. the lidar ratio), as well as for the spectral conversions between laser wavelengths.

2.3 The AERONET product

AERONET (<http://aeronet.gsfc.nasa.gov/>) is a global sunphotometric network with more than 250 stations, employing the CIMEL CE318 photometer as the standard instrument (Holben et al., 1998). In AERONET, the calibration is centralized and should be performed every 12 months, thus the instrument must be sent to specific sites (in

LIVAS: a 3-D multi-wavelength aerosol/cloud climatology

V. Amiridis et al.

[Title Page](#)

[Abstract](#)

[Introduction](#)

[Conclusions](#)

[References](#)

[Tables](#)

[Figures](#)

◀

▶

◀
Back

▶
Close

[Full Screen / Esc](#)

[Printer-friendly Version](#)

[Interactive Discussion](#)



United States or Europe) for calibration and maintenance. AERONET measurement schedule includes direct sun measurements at several wavelengths of the solar spectrum (at 380, 440, 500, 675, 870, 1020 and 1640 nm depending on the instrument type) as well as diffuse sky radiances at 440, 675, 870 and 1020 nm. Direct sun mea-

5 surements are used to retrieve the AOD at the measured wavelengths, the Ångström exponent at 440/870 nm, and fine and coarse mode optical depth at 500 nm (Holben et al., 2001; O'Neill, 2003). Direct sun and sky radiance measurements permit the retrieval of the size distribution, the complex refractive index, and the Single-Scattering Albedo (SSA; Dubovik and King, 2000; Dubovik et al., 2000; Dubovik et al., 2006).

10 3 Methods

In this section we describe the methods developed for the derivation of the multi-wavelength LIVAS climatology. The climatology is based on CALIPSO observations at 532 and 1064 nm and the converted CALIPSO extinction and backscatter product from 532 to 355, 1570 and 2050 nm, using aerosol-type-dependent spectral conversion factors derived from ground-based measurements or suitable optical models. For the 15 conversions applied in LIVAS, the spectral dependence of the extinction and backscatter is considered to follow the well-known Ångström exponential law as follows:

$$x_{\text{par}}(\lambda_2) = x_{\text{par}}(\lambda_1) \left(\frac{\lambda_1}{\lambda_2} \right)^{\dot{A}_{\lambda_1/\lambda_2}} \quad (1)$$

where $x_{\text{par}}(\lambda_2)$ is the converted extinction or backscatter at λ_2 (either 355, 1570 or 2050 nm), $\dot{A}_{\lambda_1/\lambda_2}$ is the extinction or backscatter-related Ångström exponent and $x_{\text{par}}(\lambda_1)$ is the extinction or backscatter product of CALIPSO at $\lambda_1 = 532$ nm. In the following, instead of extinction- and backscatter-related Ångström exponents we use the term “conversion factors” to describe the spectral dependence of the extinction and backscatter.

[Title Page](#)[Abstract](#)[Introduction](#)[Conclusions](#)[References](#)[Tables](#)[Figures](#)[◀](#)[▶](#)[Back](#)[Close](#)[Full Screen / Esc](#)[Printer-friendly Version](#)[Interactive Discussion](#)

[Title Page](#)[Abstract](#)[Introduction](#)[Conclusions](#)[References](#)[Tables](#)[Figures](#)[◀](#)[▶](#)[◀](#)[▶](#)[Back](#)[Close](#)[Full Screen / Esc](#)[Printer-friendly Version](#)[Interactive Discussion](#)

An overview of the methodology followed for the derivation of the aerosol-type-dependent spectral conversion factors is schematically illustrated in Fig. 1, while the aerosol model developed for LIVAS is detailed, discussed and evaluated in Sect. 3.1. The methodology for the spectral conversion of the CALIPSO Level 2 product is demonstrated through an example presented in Sect. 3.2. The section closes with the description of the processing chain followed for quality filtering and averaging the CALIPSO observations, given in Sect. 3.3.

3.1 Aerosol model for the derivation of spectral conversion factors

For the derivation of spectral conversion factors we construct the LIVAS aerosol model with typical microphysical and optical properties for each CALIPSO aerosol type. Different methods and datasets are utilized for the UV and IR spectral regions, as described in detail below.

The conversion factors for the 532 to 355 nm conversion are mainly derived from multi-wavelength EARLINET measurements of the extinction and backscatter coefficients. EARLINET measurements cannot be used for the IR conversion since the ground-based lidars of the network are spectrally limited between 355 and 1064 nm. Thus, for converting the CALIPSO backscatter and extinction products from 532 to 1570 and 2050 nm, we first define the typical size distributions and refractive indexes of the six aerosol subtypes used by CALIPSO (i.e. dust, polluted dust, smoke, marine, clean continental and polluted continental), and then we calculate the respective conversion factors utilizing well-known scattering codes like the Mie code for spherical particles (Mie, 1908; Van de Hulst, 1957), as well as the T-matrix code (Mishchenko et al., 2002) and the geometric-optics-integral-equation technique (Yang and Liou, 1996) for non-spherical particles.

The definition of representative size distributions and refractive indexes for the CALIPSO aerosol types is not a straight-forward task, mainly due to inaccuracies in the CALIPSO classification scheme (e.g., Burton et al., 2013). Aerosol classification for CALIPSO is based on a threshold algorithm that takes into account the layer-integrated

attenuated backscatter coefficient and an approximate particulate depolarization ratio as well as the surface type (either land or ocean; Omar et al., 2009). However, these properties do not provide all the information needed for unambiguously classifying the aerosol type and, as a result, misclassifications occur frequently (e.g., Burton et al., 2013).

The aerosol model in CALIPSO is introduced due to the need for a-priori knowledge of the LR, and it consists of typical size distributions and refractive indexes for each type that are retrieved by clustering AERONET measurements in respective categories/aerosol types, as described in Omar et al. (2005, 2009). Although the proposed classification is assumed to correspond to the independently derived CALIPSO aerosol types, this is not true for all cases, mainly due to the different nature of AERONET sunphotometer measurements versus CALIPSO lidar measurements used for the categorization.

In LIVAS, we initialize a number of different approaches to construct a representative aerosol model for CALIPSO and we evaluate it using the ground-based lidar measurements of EARLINET. We emphasize that in contrast to the sunphotometer-only method used for the CALIPSO aerosol model, the lidar-related methodology presented here is considered more appropriate for the CALIPSO aerosol classification scheme. This is because EARLINET performs direct ground-based lidar measurements of the backscatter coefficient in contrast to the CIMEL sunphotometer which is incapable of providing measurements at the scattering angle of 180°.

Summarizing, the LIVAS aerosol model contains the measured conversion factors from EARLINET data for the VIS-UV and the calculated conversion factors for the VIS-IR spectral range. For the latter we employ characteristic size distributions and refractive indexes from AERONET data classified into the respective aerosol types using different approaches. The results are validated against EARLINET measurements. Moreover, for aerosol types that are not probed by either EARLINET or AERONET (e.g., marine), we utilize typical properties from the Optical Properties of Aerosols and Clouds (OPAC) model (Hess et al., 1998) or other aerosol models from the literature.

Title Page	
Abstract	Introduction
Conclusions	References
Tables	Figures
◀	▶
◀	▶
Back	Close
Full Screen / Esc	
Printer-friendly Version	
Interactive Discussion	



An elaborated description of our methodology for the VIS-UV and VIS-IR spectral regions is given in Sects. 3.1.1 and 3.1.2, respectively.

3.1.1 Conversion factors in VIS-UV spectral region

For the conversion of CALIPSO aerosol backscatter and extinction from 532 to 355 nm, the aerosol-type-dependent extinction- and backscatter-related conversion factors are derived from the EARLINET database. Specifically, we use the database developed within the project “EARLINET’s Space-borne-related Activity during the CALIPSO mission” (ESA-CALIPSO; Wandinger et al., 2011). ESA-CALIPSO was an ESA-funded study aimed to establish an aerosol database from the classification of EARLINET observations performed during nearby CALIPSO overpasses with respect to the aerosol type. The methodology followed and the objectives of ESA-CALIPSO are described in Wandinger et al. (2011). In brief, during ESA-CALIPSO a large number of EARLINET observations were utilized to develop an aerosol classification scheme over Europe and to determine the respective type-dependent conversion factors and other intensive properties. Each EARLINET measurement was inspected regarding quality (e.g., noise level) and the occurrence of distinct aerosol layers. For each selected layer, an air-mass transport simulation was performed to determine its origin, transport path, and age. Additional modeling tools and satellite products (e.g., fire maps) were implemented to cross-check the sources and to assign an aerosol type for each layer (Wandinger et al., 2011).

For the derivation of the VIS to UV (532 to 355 nm) conversion factors in LIVAS, we used more than 500 aerosol layers recorded in the ESA-CALIPSO database and provided by four high-performance EARLINET stations, namely the stations of Athens, Leipzig, Potenza and Thessaloniki. The final conversion factors are calculated by averaging the measurements collected for each aerosol type. These are presented in the left column of Table 1 for backscatter (bsc) and extinction (ext).

The EARLINET measurements included in ESA-CALIPSO regarding clean marine, clean continental and stratospheric aerosol particles are limited for a reliable statisti-

Title Page

Abstract

Introduction

Conclusions

References

Tables

Figures

◀

▶

◀

▶

Back

Close

Full Screen / Esc

Printer-friendly Version

Interactive Discussion



cal analysis. The calculation of the backscatter-related conversion factors is possible, but for the extinction-related conversion factors this is not the case (mainly due to Raman lidar constraints regarding the overlap that prohibits extinction retrievals for lower marine atmospheric layers and regarding inadequate Raman returns from the stratosphere). For the aforementioned types, aerosol models provided in the literature are used in order to calculate the extinction-related conversion factors. Specifically, we use the maritime model introduced in Sayer et al. (2012) for clean marine aerosols, the OPAC model for clean continental aerosols and the stratospheric model of Wandinger et al. (1995) and Deshler et al. (1993) for stratospheric aerosols. From these models, typical size distributions and refractive indexes are retrieved and the conversion factors are calculated via the application of the Mie theory (Mie, 1908; Van de Hulst, 1957). The results are given in Table 1 (left column).

3.1.2 Conversion factors in VIS-IR spectral region

ESA-CALIPSO is mainly limited to the VIS-UV spectral region. For the VIS-IR conversions in LIVAS, we use typical size distributions and refractive indexes for each aerosol type derived from AERONET data or models, i.e. OPAC or other aerosol models in the literature. Scattering simulations are then applied for each aerosol type for the complete spectral range of LIVAS interest (i.e. 355, 532, 1064, 1570, 2050 nm). The criterion for selecting between different approaches for each aerosol type is the consistency of the calculations in the VIS-UV spectral region with the ESA-CALIPSO measurements, which are the reference for any conversion made in LIVAS. More specifically, we check the consistency of our calculations with ESA-CALIPSO for the 532-to-355-nm extinction conversion factors and the 532-to-355-nm, 1064-to-355-nm and 1064-to-532-nm backscatter conversion factors. Based on its consistency with ESA-CALIPSO, the approach selected for the derivation of the typical microphysical and optical properties of each aerosol type is described in the following:

AERONET-Omar: AERONET data are categorized with respect to the CALIPSO aerosol types based on the classification method introduced by Omar et al. (2005,

[Title Page](#)[Abstract](#)[Introduction](#)[Conclusions](#)[References](#)[Tables](#)[Figures](#)[◀](#)[▶](#)[◀](#)[▶](#)[Back](#)[Close](#)[Full Screen / Esc](#)[Printer-friendly Version](#)[Interactive Discussion](#)

2009), utilized for the construction of the CALIPSO aerosol model as described above. The difference in our approach for the LIVAS aerosol model is that for each aerosol type a consistency check with the ESA-CALIPSO data is first performed: each AERONET measurement is categorized under a specific aerosol type and the Ångström exponent at 355/532 nm and the lidar ratios at 355 and 532 nm are computed (using the phase function and the SSA provided by AERONET). Then, we reject the cases for which the aforementioned calculated optical properties are not within the range of the typical ESA-CALIPSO values for the respective aerosol type. From the constrained dataset, the average size distribution and refractive index are produced for each aerosol type and subsequently used as input in scattering calculations to produce the spectral conversion factors in the UV-IR spectral range. The method is expected to derive consistent microphysics with ESA-CALIPSO at the UV-VIS range and thus the results for the VIS-IR spectral range would be consistent.

For the scattering calculations the well-known Mie code (Mie, 1908; Van de Hulst, 1957) is applied for all the aerosol types except the non-spherical particles of dust and polluted dust, where the T-matrix code and the geometric-optics-integral-equation technique are utilized instead. More specifically, for the non-spherical scattering calculations we employ the code of Dubovik et al. (2006), which utilizes the T-matrix method for particles of size parameter smaller than 20–30 and the geometric-optics-integral-equation technique for larger particles, with size parameter up to ~ 625 . The non-spherical particles are considered as mixtures of spheroids with aspect ratios defined by a pre-defined aspect-ratio distribution, and pre-computed look-up tables are utilized, allowing fast calculations. We considered that the non-spherical particles of dust and polluted dust have the same aspect ratio distribution as the one provide for dust in Dubovik et al. (2006), which was shown to reproduce successfully the laboratory measurements of mineral dust scattering properties by Volten et al. (2001).

AERONET-CALIPSO: AERONET and CALIPSO collocated and synchronized measurements are collected, following the collocation method introduced in Schuster et al. (2012). From the collocated measurements, only those with a single CALIPSO

LIVAS: a 3-D multi-wavelength aerosol/cloud climatology

V. Amiridis et al.

[Title Page](#)

[Abstract](#)

[Introduction](#)

[Conclusions](#)

[References](#)

[Tables](#)

[Figures](#)

[◀](#)

[▶](#)

[◀](#)

[▶](#)

[Back](#)

[Close](#)

[Full Screen / Esc](#)

[Printer-friendly Version](#)

[Interactive Discussion](#)



aerosol subtype in the atmospheric column are considered. The AERONET data for these cases are subsequently classified based on the aerosol type provided by the collocated CALIPSO measurements. Scattering calculations are applied to each of the AERONET size distributions and refractive indexes of the collected cases taking into account the spherical and non-spherical part of the mixture, as this is provided by AERONET for each case.

It should be highlighted here that for this method there is no distinction between spherical and non-spherical aerosol types, instead all types are considered to contain both spherical and non-spherical particles, in accordance with the AERONET product.

- 10 The calculations for the spherical part are performed with the Mie code and for the non-spherical part with the Dubovik et al. (2006) code, following the methodology described above. For each type, all the collocated cases are averaged and from those measurements we derive the averaged values of the conversion factors.

15 The dataset is not constrained with ESA-CALIPSO as in the AERONET-Omar approach. This is due to the fact that the specific approach aims to deliver typical conversion factors for the aerosol types classified by the CALIPSO classification scheme itself, thus no correspondence to the nature of the atmospheric aerosol loads is required.

20 **OPAC:** a typical size distribution and refractive index are extracted from the OPAC dataset for each aerosol type, considering typical ambient conditions of 70 % relative humidity. We derive the conversion factors by performing scattering calculations with the Mie code.

25 **Approaches taken from the literature:** the studies of Wandinger et al. (1995) and Deshler et al. (1993) provide a range of typical size distributions and refractive indexes for the stratospheric aerosol, while the marine model of Sayer et al. (2012) provides a typical size distribution and refractive index for marine aerosol. We derive the conversion factors by performing scattering calculations with the Mie code.

LIVAS: a 3-D multi-wavelength aerosol/cloud climatology

V. Amiridis et al.

[Title Page](#)

[Abstract](#)

[Introduction](#)

[Conclusions](#)

[References](#)

[Tables](#)

[Figures](#)

◀

▶

◀
Back

▶
Close

[Full Screen / Esc](#)

[Printer-friendly Version](#)

[Interactive Discussion](#)



3.1.3 LIVAS aerosol model evaluation against ESA-CALIPSO database

As already mentioned, the aim of the LIVAS aerosol model is to reproduce spectral conversion factors that are consistent with ESA-CALIPSO, a reference database of measured lidar-related aerosol properties, especially regarding the backscatter coefficient, the lidar ratio, and the spectral dependence of the backscatter. While the conversion factors for the VIS-UV spectral range are derived directly from the ESA-CALIPSO database, the VIS-IR calculated conversion factors are not always consistent with the database values. Therefore, for each aerosol type we select the VIS-IR methodology that provides compatible results with the ESA-CALIPSO for the VIS-UV conversion factors. In this way we ensure the best possible consistency of the conversion factors for the entire spectral range.

Our final results are presented and discussed herein: Figure 2 shows the calculated conversion factors using all the approaches described above and their comparison with ESA-CALIPSO at VIS-UV. The selected approach for each aerosol type is denoted in Fig. 2 with large size symbols. Starting from the AERONET-Omar approach, we found that it performed better when compared to ESA-CALIPSO for the polluted continental type, resulting in a very good agreement for the extinction conversion factor and best performance regarding the backscatter conversion. For the other types this approach reproduces well the extinction-related conversion factors. However, the backscatter-related conversion factors for these types could not be reproduced such as to fit the ESA-CALIPSO acceptable range of values. We believe that the discrepancies in backscatter spectral dependence observed for most of the aerosol types in the AERONET-Omar approach are most likely due to the fact that AERONET lacks the capability to directly measure in the backscattering direction. Comparisons found in the literature between Raman-lidar-measured and photometer-retrieved lidar ratio, reinforce this argument (e.g., Mueller et al., 2007).

Dust and polluted dust aerosols are most likely classified correctly by CALIPSO due to its polarization sensitivity (e.g., Burton et al., 2013; Amiridis et al., 2013). For this

Title Page	
Abstract	Introduction
Conclusions	References
Tables	Figures
◀	▶
◀	▶
Back	Close
Full Screen / Esc	
Printer-friendly Version	
Interactive Discussion	



reason, we choose the AERONET-CALIPSO approach for the calculation of their conversion factors. The approach shows a relatively better agreement with ESA-CALIPSO compared to the AERONET-Omar approach, especially for the backscatter-related conversion factors (Fig. 2). It should be noted though that the evaluation of the retrieved values with ESA-CALIPSO for polluted dust is only indicatory. This is because CALIPSO assumes the same properties for any kind of dust mixture (e.g., dust-smoke, dust-marine), while ESA-CALIPSO shows that the optical properties are highly variable for different dust mixtures. Specifically, ESA-CALIPSO provides intensive properties for mixtures of dust with polluted continental, smoke and marine aerosol separately and what we use here in order to compare with CALIPSO is an average of these properties.

For smoke aerosols the AERONET-CALIPSO approach shows similar results as AERONET-Omar, performing well for the extinction conversion factors, but failing to reproduce the ESA-CALIPSO backscatter conversion factors (Fig. 2). For this aerosol type we choose to include in the LIVAS model the calculated conversion factors from the AERONET-CALIPSO approach. This decision was based on the fact that the classification of smoke by CALIPSO is the most uncertain compared to the other aerosol types, as reported by Burton et al. (2013). The authors of this study report a percentage agreement of 13 % for smoke classification when comparing with airborne HSRL classification results. Smoke misclassification was also found to be the reason of the discrepancies between CALIPSO and AERONET reported in Schuster et al. (2012) in terms of AOD measurements. These findings indicate that the CALIPSO smoke classification may not correspond to real smoke presence, thus the properties of this CALIPSO classification category may not be comparable with real smoke detections by ESA-CALIPSO. Thus, we prefer to use the calculations for CALIPSO smoke coincidences (AERONET-CALIPSO approach), ignoring the ESA-CALIPSO smoke statistics.

For clean marine and clean continental aerosol, the ESA-CALIPSO database does not contain an adequate number of measurements to provide statistically significant averages. AERONET data also suffer from the small number of clean marine and clean continental cases. Thus, for clean marine we use the size distribution and refractive

LIVAS: a 3-D multi-wavelength aerosol/cloud climatology

V. Amiridis et al.

[Title Page](#)

[Abstract](#)

[Introduction](#)

[Conclusions](#)

[References](#)

[Tables](#)

[Figures](#)

◀

▶

[Back](#)

[Close](#)

[Full Screen / Esc](#)

[Printer-friendly Version](#)

[Interactive Discussion](#)



index provided in the maritime model of Sayer et al. (2012) and for clean continental we use the ones provided in the OPAC database. Note that the size distribution and refractive index for clean continental aerosol from OPAC database are considered at ambient conditions of 70 % relative humidity.

- 5 Finally, for the stratospheric aerosol type we use the model introduced in Deshler et al. (1993) and Wandinger et al. (1995). The conversion factors found to be in good agreement with ESA-CALIPSO values (not shown in Fig. 2).

10 The final aerosol-type-dependent VIS-IR conversion factors used in LIVAS are presented in the right panel of Table 1 for extinction (ext) and backscatter (bsc). Overall, as seen in Fig. 2, the LIVAS aerosol model in the VIS-IR is compatible with ESA-CALIPSO in the VIS-UV spectral region regarding the extinction-related conversion factors. However, the agreement with regard to the VIS-UV backscatter-related conversion factors is not that satisfactory. For the extinction and backscatter-related conversion factors in 15 the IR, one point of concern is the extrapolation of the refractive index at the longer wavelengths, since this information is not provided from AERONET.

3.1.4 Comparison of LIVAS and CALIPSO aerosol models

The microphysical properties used for calculating the VIS-IR conversion factors are compared in this section with the ones in the CALIPSO aerosol model (Omar et al., 2005, 2009). Figure 3 shows the comparison of LIVAS versus CALIPSO size distributions for each aerosol type, while Figs. 4, 5 and 6 show the spectral dependence 20 of the complex refractive index and the SSA, respectively, at LIVAS wavelengths for the two models. Figure 7 shows the backscatter and extinction conversion factors at 355/532 nm, the lidar ratio at 532 nm and the effective radius for the LIVAS and CALIPSO aerosol models, compared with the ones provided in the ESA-CALIPSO database.

In Fig. 3 the best agreement between the LIVAS and the CALIPSO model size distributions is found for the polluted continental type. For smoke particles the CALIPSO model considers the same volume for fine and coarse particles, whereas the LIVAS

LIVAS: a 3-D multi-wavelength aerosol/cloud climatology

V. Amiridis et al.

[Title Page](#)

[Abstract](#)

[Introduction](#)

[Conclusions](#)

[References](#)

[Tables](#)

[Figures](#)

◀

▶

◀
Back

▶
Close

[Full Screen / Esc](#)

[Printer-friendly Version](#)

[Interactive Discussion](#)



model presents a domination of the fine mode. The latter agrees well with the averaged size distribution of smoke type provided in Dubovik et al. (2002) AERONET eight-year climatology and is considered more typical as it is supported by other studies as well as (Reid et al., 2005; Eck et al., 1999, 2003). For dust type the LIVAS size distribution has fewer fine particles than the CALIPSO model, in agreement with the AERONET climatology of Dubovik et al. (2002) and findings of experimental campaigns dedicated to mineral dust characterization (e.g., McConnell et al., 2008; Weinzierl et al., 2009; Müller et al., 2011; Toledano et al., 2011). For the polluted dust type both models seem to fall within the range of the large variability reported in the literature for dusty mixtures (Eck et al., 1999; Jung et al., 2010). The more pronounced fine mode in the LIVAS model resembles the size distributions of dust and pollution mixtures (Kim et al., 2007). However, an extensive discussion on the polluted dust type is avoided here since there is no clear definition of the non-dust components for this type in the CALIPSO model. LIVAS size distribution for clean marine type is based on the maritime model of Sayer et al. (2012). Similar size distributions for marine particles are provided in other studies as well (e.g., Dubovik et al., 2002; Smirnov et al., 2002). The largest disagreement is seen for the clean continental type. We believe that the pronounced fine mode in the LIVAS size distribution from OPAC is due to the hygroscopic growth of the hydrophilic fine particles in ambient relative humidity of 70 %. However, the clean continental type in global CALIPSO records has a contribution of the order of 2 %, making this type of less importance for LIVAS climatology. For the aerosol model though, a better definition of the aerosol components of this type should be considered.

Regarding the differences on the refractive index assumed by LIVAS and CALIPSO aerosol models, these are presented in Figs. 4 and 5, respectively for the reader's reference. We also present a comparison of the LIVAS and CALIPSO SSA in Fig. 6. The comparison shows an overall disagreement in the SSA between the two aerosol models. We should note here that Omar et al. (2009) provide the refractive index values at 532 and 1064 nm and we used linear extrapolation to construct the CALIPSO aerosol model for all the wavelengths of LIVAS (see Figs. 4 and 5). Despite the dis-

LIVAS: a 3-D multi-wavelength aerosol/cloud climatology

V. Amiridis et al.

[Title Page](#)

[Abstract](#)

[Introduction](#)

[Conclusions](#)

[References](#)

[Tables](#)

[Figures](#)

[◀](#)

[▶](#)

[◀](#)

[▶](#)

[Back](#)

[Close](#)

[Full Screen / Esc](#)

[Printer-friendly Version](#)

[Interactive Discussion](#)



agreement of the SSA values, their spectral slope is similar for all the types (except the clean continental aerosol) for both models. Even more so, for polluted continental, dust, smoke and clean marine particles the spectral slope of the SSA agrees relatively well with the corresponding ones provided in Dubovik et al. (2002) climatology. More specifically, for the dust type the spectral slope of the SSA for both models is flatter but it closely resembles the one presented in Dubovik et al. (2002), as well as in other studies (Müller et al., 2011; Toledano et al., 2011). For smoke, the absorption has to do mainly with the black carbon content and can greatly vary (Eck et al., 2003). The spectral dependence and range of SSA values in LIVAS model are similar with the values provided in Dubovik et al. (2002) climatology and references therein, whereas the CALIPSO model presents lower values, which although agree with other studies (e.g., Eck et al., 1998, 2003). The polluted dust SSA spectral dependence is similar for both models, but different than of dust mixtures with smoke and pollution presented in the literature (e.g., Jung et al., 2010; Holler et al., 2003). Finally, the clean marine SSA for both models agrees very well with other studies in the literature (e.g., Dubovik et al., 2002; Hasekamp et al., 2011).

In Fig. 7, a final comparison between ESA-CALIPSO, LIVAS and CALIPSO aerosol models is given in terms of extinction and backscatter conversion factors, lidar ratio at 532 nm and effective radius. The extinction and backscatter conversion factors at 355/532 nm for the CALIPSO aerosol model are not provided by Omar et al. (2009) and instead they are calculated using the size distribution and refractive index of the CALIPSO model. For the scattering calculations we used the Mie code for the types with spherical particles and the Dubovik software for the non-spherical particles of dust and polluted dust types. The methodology is the same as the one described for the AERONET-Omar approach in Sect. 3.1.2. The lidar ratio at 532 nm is taken directly from what is reported in Omar et al. (2009), while due to the fact that the effective radius is not given in this work, it is calculated from the size distribution for each type therein. The maximum deviation is found for the backscatter conversion factors, especially for the dust type (either pure or mixed; Fig. 7 upper-right). It is a possibil-

LIVAS: a 3-D multi-wavelength aerosol/cloud climatology

V. Amiridis et al.

[Title Page](#)

[Abstract](#)

[Introduction](#)

[Conclusions](#)

[References](#)

[Tables](#)

[Figures](#)

◀

▶

[Back](#)

[Close](#)

[Full Screen / Esc](#)

[Printer-friendly Version](#)

[Interactive Discussion](#)



- ity that one of the reasons of these discrepancies is the lower effective radius produced from the large fine-mode contribution in the size distribution assumed in Omar et al. (2009). For polluted continental aerosol we get a relatively good agreement for the LIVAS and CALIPSO models, in accordance with the ESA-CALIPSO data as well.
- 5 For smoke aerosol the agreement is also good for both models, but both are not consistent with the ESA-CALIPSO for the backscatter conversion. For clean marine and clean continental aerosol the LIVAS model agrees well with ESA-CALIPSO, but this is not the case for the CALIPSO model. Overall, we found that the LIVAS and CALIPSO aerosol models agree only for the polluted continental aerosols, whereas for the rest of
- 10 the aerosol types the LIVAS model to be closer to the ESA-CALIPSO measured values than the CALIPSO model.

3.1.5 Spectral conversions for other LIVAS products

Depolarization spectral conversions have not been applied in LIVAS since multi-wavelength depolarization measurements are rare and available only during experimental campaigns (Freudenthaler et al., 2009; Groß et al., 2011a, b), thus the dataset is not considered statistically significant. A single-wavelength depolarization climatology is provided in LIVAS using CALIPSO Level 2 particle depolarization ratio averages at 532 nm.

Furthermore, a global cloud climatology is given based on CALIPSO observations at 20 532 nm. With respect to clouds, the wavelength conversion is most probably of minor importance due to approximately neutral scattering behavior along the range of LIVAS wavelengths.

In addition, a climatology for the stratospheric features detected by CALIPSO is provided, separated to cloud and aerosol features. Specifically, the stratospheric features 25 detected by CALIPSO are separated in polar stratospheric clouds and stratospheric aerosols using the temperature threshold technique proposed by Pitts et al. (2009). In brief, we classify stratospheric features as Polar Stratospheric Clouds (PSCs) when the temperature is lower than 198 K, while features of higher temperatures are classified

LIVAS: a 3-D multi-wavelength aerosol/cloud climatology

V. Amiridis et al.

[Title Page](#)

[Abstract](#)

[Introduction](#)

[Conclusions](#)

[References](#)

[Tables](#)

[Figures](#)

◀

▶

◀

▶

[Back](#)

[Close](#)

[Full Screen / Esc](#)

[Printer-friendly Version](#)

[Interactive Discussion](#)



as stratospheric aerosols. The separation is applied only for stratospheric features at latitudes greater than 54° N and less than -54° S, while for the latitudes in between, the stratospheric features are considered as aerosols.

Finally, a set of selected scenes of specific atmospheric phenomena (e.g., dust outbreaks, volcanic eruptions, wild fires, polar stratospheric clouds) is produced. The conversion factors for the selected scenes are delivered after thorough investigation of each case study, based on CALIPSO-collocated ground-based measurements that are reported to the literature. Whenever this is not possible (as for the IR conversion), the LIVAS climatological conversion factors are used.

10 3.2 Example for the spectral conversion of single CALIPSO profiles

The obtained aerosol-type-dependent conversion factors for VIS-to-UV and VIS-to-IR are applied to the CALIPSO Level 2 product at 532 nm for the respective aerosol layer type inferred by the CALIPSO aerosol classification scheme. An example of the conversion from 532 to 355 nm is presented in Fig. 8. Each CALIPSO layer in the profile 15 example is converted from 532 to 355 nm using the LIVAS 532/355 extinction-related conversion factor, depending on the aerosol type retrieved by the CALIPSO aerosol classification scheme for the layer. In the example presented in Fig. 8, LIVAS extinction-related conversion factors for clean marine (0.78), dust (0.55) and polluted continental (1.24) types are applied to the CALIPSO extinction coefficient at 532 nm, based on the 20 Ångström exponential law described in Eq. (1).

3.3 CALIPSO quality filtering and averaging processing chain

For the production of the final LIVAS products, we use the methodology developed by the CALIPSO team for the Level 3 aerosol product, as described in Winker et al. (2013). Our algorithm has been tested for reproducing the CALIPSO Level 3 product, which is 25 an aggregation onto a global 2×5 degree latitude-longitude grid. After the positive evaluation of the averaging procedure (not shown here), we applied it on Level 2 CALIPSO

LIVAS: a 3-D multi-wavelength aerosol/cloud climatology

V. Amiridis et al.

[Title Page](#)

[Abstract](#)

[Introduction](#)

[Conclusions](#)

[References](#)

[Tables](#)

[Figures](#)

◀

▶

◀

▶

[Back](#)

[Close](#)

[Full Screen / Esc](#)

[Printer-friendly Version](#)

[Interactive Discussion](#)



profiles at 532 and 1064 nm but also on the corresponding LIVAS spectrally converted profiles at 355, 1570 and 2050 nm in order to derive 1×1 degree latitude-longitude averaged vertical distributions. The vertical resolution of the LIVAS product is identical to CALIPSO Level 3, namely 60 m in the tropospheric region between the surface and 5 20 km and 180 m in the stratospheric region between 20 and 30 km.

As input to the averaging algorithm, we use the Version 3 CALIOP Level 2 aerosol profile product, which is quality screened prior to averaging, to eliminate samples and layers that are detected or classified with very low confidence, or that contain untrustworthy extinction retrievals. In brief, the filters concern the Cloud-Aerosol Discrimination 10 (CAD) score, Extinction Quality Control (QC) flag, aerosol extinction uncertainty, isolated 80 km layer, misclassified cirrus, undetected surface attached aerosol low bias, large negative near-surface extinction, surface contamination beneath surface-attached opaque layer, removal of samples below opaque cloud and aerosol layers. Detailed explanation of the methodology followed for the production of the Level 3 15 product and respective filtering and flags, is provided in the Appendix of Winker et al. (2013). For the particle linear depolarization, an extra filter is applied in LIVAS in order to average this parameter for the same samples collected for the extinction. For that, we average only particle linear depolarization CALIPSO retrievals for which the extinction uncertainty is less than 99.9 km^{-1} , so as to maintain the same measurement 20 sampling. For the quality screening of cloud and stratospheric feature profiles a similar methodology is followed.

In the CALIPSO Level 3 product, four types of products are generated each month, depending on sky condition and temporal coverage, and are separated into day/night segments. In LIVAS, only the “combined” product is used (Winker et al., 2014) in order 25 to achieve better quality of aerosol climatology regarding cloud discrimination and measurement accuracy. Moreover, beyond the mean extinction profiles for the total aerosol load, LIVAS provides mean extinction profiles at 532 nm for each of the six aerosol types in the CALIPSO classification scheme. Finally, the seasonal distribution

LIVAS: a 3-D multi-wavelength aerosol/cloud climatology

V. Amiridis et al.

[Title Page](#)

[Abstract](#)

[Introduction](#)

[Conclusions](#)

[References](#)

[Tables](#)

[Figures](#)

◀

▶

◀

▶

[Back](#)

[Close](#)

[Full Screen / Esc](#)

[Printer-friendly Version](#)

[Interactive Discussion](#)



of the vertical distribution of the extinction for each LIVAS cell is provided. A schematic outline of the LIVAS processing chain is given in Fig. 9.

4 Results and discussion

4.1 LIVAS products

- 5 The final LIVAS climatology contains multi-wavelength 4-year averaged vertical distributions and statistics for a global grid of $1 \times 1^\circ$. Here, we demonstrate the LIVAS products through an example for one grid cell corresponding to our hometown, Athens, in Greece (centroid latitude of 38.5° N and longitude of 23.5° E).

In the upper panel of Fig. 10 the aerosol extinction is given for the LIVAS lidar wavelengths, i.e. 355, 532, 1064, 1570, 2050 nm, along with the standard deviation of the averaging at 532 nm (grey line). The number of observations is presented in the right panel for each plot, in order to have a measure of the representativeness of the mean aerosol extinction for each cell, which depends on the available CALIPSO overpasses and corresponding samples. The maximum surface elevation over the CALIPSO overpass is given for the grid cell of interest, as obtained from the digital elevation map (DEM) used by CALIPSO. In the middle panel of Fig. 10, the mean extinction profile is given per CALIPSO aerosol type, while in the lower panel the mean extinction is given per season with the corresponding sampling/occurrences used for their production.

Additional LIVAS products are provided for particle depolarization at 532 nm. These refer to the mean particle depolarization along with its standard deviation (Fig. 11 – upper panel). Moreover, mean cloud extinction at 532 nm is given in LIVAS (Fig. 11 – middle panel) along with mean extinction coefficient of stratospheric features in total (Fig. 11 – lower panel) but also for PSCs and aerosol particles separately.

Finally, for each grid cell a number of statistical parameters are provided in LIVAS regarding the mean, minimum and maximum surface elevation, the number of overpasses for each cell, the number of examined profiles, the samples averaged after

Title Page

Abstract

Introduction

Conclusions

References

Tables

Figures

◀

▶

Back

Close

Full Screen / Esc

Printer-friendly Version

Interactive Discussion



filtering (total, aerosol, clear air), the subtype occurrence in the aerosol total observations (in percentages) and the AOD at 532 nm (mean, median and standard deviation).

4.2 LIVAS AOD evaluation

In this section an evaluation of the LIVAS climatological AOD mean values at 532 nm is given, using collocated AERONET AOD averages. AERONET stations included in each grid cell of $1 \times 1^\circ$ are considered representative when the stations are operated for the same time period with LIVAS (2008–2011). LIVAS mean AOD is calculated by the integration of the 4-year-averaged extinction profile, while AERONET AOD is calculated by averaging all available station data. A first comparison of LIVAS AODs against AERONET is presented in Fig. 12. Blue circles denote the absolute value of the difference (LIVAS mean – AERONET mean), while the red crosses denote the elevation difference between the AERONET site and the mean elevation of the CALIPSO ground track. This map provides only positive biases (absolute values) to demonstrate the range of discrepancies with respect to the elevation slope. Large differences can also be attributed to specific grid cell under-sampling by CALIPSO in the 4-year period, as discussed below.

Large elevation differences may cause large AOD biases since in such cases the optical path lengths monitored by AERONET and CALIPSO instruments can vary. Moreover, when CALIPSO overpasses high-slope terrains, the sampling may become inadequate for heights lower than the maximum elevation. An example of such a case is given in Fig. 13 for the AERONET station of “ND_Marbel_Univ” in Philippines. CALIPSO overpasses this station over elevations ranging from zero to 1.46 km. The number of observations for heights lower than the maximum elevation becomes very small (Fig. 13 – right panel) and inadequate for statistical purposes. This under-sampling affects the final averaged extinction profile as shown in the left panel of Fig. 13 for heights lower than the maximum elevation. In order to eliminate these effects from the comparison of LIVAS with AERONET, we apply on our dataset the following constraints:

[Title Page](#)

[Abstract](#)

[Introduction](#)

[Conclusions](#)

[References](#)

[Tables](#)

[Figures](#)

◀

▶

◀
Back

▶
Close

[Full Screen / Esc](#)

[Printer-friendly Version](#)

[Interactive Discussion](#)



1. The elevation difference between the AERONET site and CALIPSO mean ground track elevation is kept below 100 m.
2. The elevation slope in CALIPSO overpass is constrained to be less than 400 m.
3. CALIPSO sampling is controlled by constraining the comparison over grid cells with large number of overpasses, i.e. over 150.

5

The third constraint is considered crucial for the representativeness of LIVAS climatological values in general. As shown in Fig. 14, in approximately 30 % of the global $1 \times 1^\circ$ cells of the climatology, the number of overpasses is less than 150. This undersampling along with possible high-slope terrains can cause unrealistic results.

10

Figure 15 presents the absolute bias of the means for our constrained dataset (i.e. averaged CALIPSO AOD minus the averaged AERONET AOD). For most sites the comparison reveals biases within ± 0.1 in terms of AOD. Negative LIVAS biases lower than -0.1 (denoted in Fig. 15 with blue color) are found mostly over the Saharan desert, a result that may be related to possible CALIPSO underestimations for dust as already reported in the literature (e.g., Wandinger et al., 2010; Schuster et al., 2012; Tesche et al., 2013; Amiridis et al., 2013). Positive LIVAS biases larger than 0.1 denoted with red color in Fig. 15 are mostly found over coastlines. This effect is not well understood yet. Campbell et al. (2012) found CALIPSO offsets over coastlines when comparing with the US Naval Aerosol Analysis and Predictive System (NAAPS). Recently, Kanitz et al. (2014) found a systematic overestimation of the AOD over land in coastal areas of up to a factor of 3.5. The researchers attribute the possible CALIPSO overestimation to the surface-dependent criterion (land/ocean) included in the classification scheme which may prohibit a correct classification of sea-breeze-related marine aerosol over land, leading to unrealistically high lidar ratio assumptions.

15

We have to mention here that the LIVAS validation presented in Fig. 15 cannot be conclusive on the aforementioned possible issues. Overall, the global LIVAS agreement with AERONET within 0.1 AOD is considered a very good result for a 4-year climatological product. Keeping the constrained dataset for a quantitative comparison,

LIVAS: a 3-D multi-wavelength aerosol/cloud climatology

V. Amiridis et al.

[Title Page](#)[Abstract](#)[Introduction](#)[Conclusions](#)[References](#)[Tables](#)[Figures](#)[◀](#)[▶](#)[◀](#)[▶](#)[Back](#)[Close](#)[Full Screen / Esc](#)[Printer-friendly Version](#)[Interactive Discussion](#)

we present in Fig. 16 scatter plots for AOD averages at the different LIVAS wavelengths. In the upper panel we show the comparison for the averaged AOD at 532 nm (left) and for the standard deviation of the distribution (right). A Pearson correlation coefficient of 0.86 reveals a very good agreement for the AOD at 532 nm. The slope of the linear regression is 0.79, showing a slight underestimation of the LIVAS AOD. Since the 532 nm LIVAS products come directly from CALIPSO averages, this underestimation is probably related to CALIPSO limitations (e.g., Schuster et al., 2012; Omar et al., 2013). The variability of the CALIPSO samples averaged for LIVAS is consistent with AERONET as shown in the upper right panel of Fig. 16. The LIVAS AOD at 355 nm (lower left panel) is also in a very good agreement with AERONET, showing similar values of Pearson's r and slope as those of the 532 nm comparison. This result shows that the conversion of the CALIPSO extinction product from 532 to 355 nm has been successful using the EARLINET conversion factors. Regarding the comparison at IR wavelengths (lower right panel), the results are not encouraging. LIVAS AOD at 1570 nm is consistent with AERONET for AODs lower than 0.1 but not for higher values where LIVAS heavily underestimates. This can be attributed to errors introduced due to the extrapolation of the AERONET AOD in the IR (note that we use AERONET AOD measurements at 440, 670, 860 and 1020 nm), and/or to uncertainties introduced by the LIVAS conversion scheme in the IR.

20 4.3 LIVAS web-portal

The LIVAS climatology is freely available under the url: <http://lidar.space.noa.gr:8080/livas/>, where the database is stored and exposed (Fig. 17). The webpage provides the complete information on the methodological approaches and instructions on portal's usage. The data are provided in ASCII and netcdf formats, while brief statistics and quick-view charts are projected online. The user can select to download the database via ftp, or navigate to the region of interest by using a dynamic map to select over the World grid of 1×1 degree spatial resolution. The map provides the possibility to overlay a layer that represents the number of CALIPSO overpasses. This is considered crucial

LIVAS: a 3-D multi-wavelength aerosol/cloud climatology

V. Amiridis et al.

[Title Page](#)

[Abstract](#)

[Introduction](#)

[Conclusions](#)

[References](#)

[Tables](#)

[Figures](#)

◀

▶

[Back](#)

[Close](#)

[Full Screen / Esc](#)

[Printer-friendly Version](#)

[Interactive Discussion](#)



for the use of the database since only grid cells with a number of CALIPSO overpasses greater than 150 are recommended for their statistical representativeness. Moreover, the user can overlay global AODs or cloud optical depths on the map. In the example of Fig. 18, the global distribution of LIVAS AODs is presented, showing high values over well-known sources like the dust belt, India and China as well as transport paths as the one from Sahara westward across the Atlantic.

5 Summary and conclusions

We presented LIVAS, a 4-year multi-wavelength global aerosol and cloud optical climatology that has been developed for complementing existing datasets used by ESA

for instrument performance simulation of current and future space-borne lidars as well as retrieval algorithm testing activities based on realistic atmospheric scenarios. In order to cover the different spectral domains for HSRL and IPDA lidars, the compiled database addresses the three harmonic operating wavelengths of Nd-YAG lasers (355, 532 and 1064 nm) as well as typical wavelengths of IPDA lidars in the SWIR spectral domain (1570 and 2050 nm).

When compared to AERONET, the LIVAS AOD climatological values appear to be realistic and representative for VIS wavelengths but also for UV, making this climatology appropriate for use by ADM-Aeolus and EarthCARE. Regarding the IR conversion however, LIVAS is not considered representative when compared to AERONET, especially for AODs higher than 0.1. We believe that LIVAS is representative in the UV due to the fact that the conversion factors were provided by ground-based lidar measurements of high quality as those provided by EARLINET. Moreover, the methodology used for the application of the conversions has been based on aerosol classification advances developed within the ESA-CALIPSO project. For IR however, the conversion factors were not measured but they were calculated from scattering simulations using typical size distributions and refractive indexes assumed for each CALIPSO aerosol type, deduced from AERONET data and aerosol models provided in the literature. Even though

LIVAS: a 3-D multi-wavelength aerosol/cloud climatology

V. Amiridis et al.

[Title Page](#)

[Abstract](#)

[Introduction](#)

[Conclusions](#)

[References](#)

[Tables](#)

[Figures](#)

[◀](#)

[▶](#)

[◀](#)
[Back](#)

[▶](#)
[Close](#)

[Full Screen / Esc](#)

[Printer-friendly Version](#)

[Interactive Discussion](#)



EARLINET was used to constrain the IR simulations, the final results are not satisfactory and more work is needed that would benefit from potential future IR ground-based measurements. However, the LIVAS aerosol model found to be more consistent with ESA-CALIPSO but also the relative literature than the one used by CALIPSO for the
5 VIS-UV spectral region.

In the future, we plan to expand LIVAS in monthly-averaged aggregations in order to provide timeseries for UV lidar products. In this way, LIVAS timeseries could be homogenized in the future with EarthCARE products for the consolidation of a multi-year aerosol/cloud multi-wavelength 4-D dataset appropriate for climate studies. However,
10 the challenges for this task are significant, due to a number of open scientific questions and related knowledge gaps. Specifically, the homogenization scheme envisaged cannot be realized without defining a common aerosol/cloud model that will be applicable to all the missions. This includes also the definition of a common aerosol/cloud classification scheme for the space-borne products and ancillary ground-based datasets and
15 the derivation of aerosol/cloud-type-dependent spectral conversion factors for all lidar-related properties, i.e. extinction, backscatter and depolarization. It is believed that the well-established EARLINET network offers a unique opportunity to support such an effort. Several EARLINET stations operate multi-wavelength Raman lidars, with most of them measuring particle depolarization as well. Network's so-called "core stations"
20 deliver the entire CALIOP/ALADIN/ATLID parameter set, so that conversion factors for a variety of aerosol types can be derived experimentally over a comparably long time period.

Acknowledgements. This work has been developed under the auspices of the ESA-ESTEC project: Lidar Climatology of Vertical Aerosol Structure for Space-Based LIDAR Simulation
25 Studies (LIVAS) contract no. 4000104106/11/NL/FF/fk. The publication was supported by the European Union Seventh Framework Programme (FP7-REGPOT-2012-2013-1), in the framework of the project BEYOND, under Grant Agreement no. 316210 (BEYOND – Building Capacity for a Centre of Excellence for EO-based monitoring of Natural Disasters). The research leading to these results has received funding from the European Union Seventh Framework
30 Programme (FP7/2007-2013) under grant agreement no. 262254 (ACTRIS), grant agreement

LIVAS: a 3-D multi-wavelength aerosol/cloud climatology

V. Amiridis et al.

[Title Page](#)

[Abstract](#)

[Introduction](#)

[Conclusions](#)

[References](#)

[Tables](#)

[Figures](#)

[◀](#)

[▶](#)

[◀](#)
[▶](#)

[◀](#)
[▶](#)

[Back](#)

[Close](#)

[Full Screen / Esc](#)

[Printer-friendly Version](#)

[Interactive Discussion](#)



no. 606953 and grant agreement no. 289923 – ITaRS. This research has been financed by EPAN II and PEP under the national action “Bilateral, multilateral and regional R&T cooperations” (AEROVIS Sino-Greek project). This publication was supported by the “Development Proposals of Research Entities – KRIPIS”, which is funded by N.P. “Competitiveness and Entrepreneurship”, Action: “PROTEAS – Advanced Space Applications for the Exploration of the Universe, Space and Earth”.

The authors acknowledge EARLINET for providing aerosol lidar profiles available under the World Data Center for Climate (WDCC) (“The EARLINET publishing group 2000–2010, 2014a, b, c, d, e”). We thank the AERONET PIs and their staff for establishing and maintaining the AERONET sites used in this investigation. CALIPSO data were obtained from the ICARE Data Center (<http://www.icare.univ-lille1.fr/>). We would like to thank Jason Tackett for his support during the algorithm development for the production of Level 3 CALIPSO products.

References

- Amiridis, V., Wandinger, U., Marinou, E., Giannakaki, E., Tsekeri, A., Basart, S., Kazadzis, S., Gkikas, A., Taylor, M., Baldasano, J., and Ansmann, A.: Optimizing CALIPSO Saharan dust retrievals, *Atmos. Chem. Phys.*, 13, 12089–12106, doi:10.5194/acp-13-12089-2013, 2013.
- Böckmann, C., Wandinger, U., Ansmann, A., Bösenberg, J., Amiridis, V., Boselli, A., Delaval, A., De Tomasi, F., Frioud, M., Grigorov, I. V., Hågård, A., Horvat, M., Iarlöri, M., Komguem, L., Kreipl, S., Larchevêque, G., Matthias, V., Papayannis, A., Pappalardo, G., Rocadenbosch, F., Rodrigues, J. A., Schneider, J., Shcherbakov, V., Wiegner, M.: Aerosol lidar intercomparison in the framework of the EARLINET project. 2. Aerosol backscatter algorithms, *Appl. Opt.*, 43, 977–989, 2004.
- Bösenberg, J., Linné, H., Matthias, V., Böckmann, C., Mironova, I., Schneidenbach, L., Kirsche, A., Mekler, A., Wiegner, M., Freudenthaler, V., Stachlewska, I., Kumpf, W., Pappalardo, G., Amodeo, A., Mona, L., Pandolfi, M., Balis, D., Amoridris, V., Zerefos, C., Ansmann, A., Mattis, I., Wandinger, U., Müller, D., Spinelli, N., Wang, X., Boselli, A., Chaikovsky, A., Comeron, A., Rocadenbosch, F., Pérez, C., Baldasano, J.M., Pelon, J., Sauvage L., Perrone, R.M., De Tomasi, F., Eixmann, R., Mitev, V., Matthey , R., Hagard, A., Persson, R., Carlsson G., Rizi, V., Iarlöri, M., Vaughan, G., Trickl, T., Kreipl, S., Giehl, H., Simeonov, V., Resendes, D.P., Rodrigues, J. A., Sobolewski, P., Nickovic, S., Zavrtanik, M., Stoyanov, D., Grigorov, I.,

LIVAS: a 3-D
multi-wavelength
aerosol/cloud
climatology

V. Amiridis et al.

Title Page

Abstract

Introduction

Conclusions

References

Tables

Figures

◀

▶

◀

▶

Back

Close

Full Screen / Esc

Printer-friendly Version

Interactive Discussion



- Kolarov, G., and Papayannis, A.: EARLINET: A European Aerosol Research Lidar Network to Establish an Aerosol Climatology, Max-Planck-Institut Report No. 348, 2003.
- Burton, S. P., Ferrare, R. A., Vaughan, M. A., Omar, A. H., Rogers, R. R., Hostetler, C. A., and Hair, J. W.: Aerosol classification from airborne HSRL and comparisons with the CALIPSO vertical feature mask, *Atmos. Meas. Tech.*, 6, 1397–1412, doi:10.5194/amt-6-1397-2013, 2013.
- Campbell, J. R., Reid, J. S., Westphal, D. L., Zhang, J., Tackett, J. L., Chew, B. N., Welton, E. J., Shimizu, A., Sugimoto, N., Aoki, K., and Winker, D. M.: Characterizing the vertical profile of aerosol particle extinction and linear depolarization over Southeast Asia and the Maritime Continent: the 2007–2009 view from CALIOP, *Atmos. Res.*, 122, 520–543, doi:10.1016/j.atmosres.2012.05.007, 2012.
- Deshler, T., Johnson, B. J., and Rozier, W. R.: Balloonborne measurements of Pinatubo aerosol during 1991 and 1992 at 41° N: vertical profiles, size distribution, and volatility, *Geophys. Res. Lett.*, 20, 1435–1438, 1993.
- Dubovik, O. and King, M. D.: A flexible inversion algorithm for retrieval of aerosol optical properties from sun and sky radiance measurements, *J. Geophys. Res.*, 105, 20673–20696, 2000.
- Dubovik, O., Smirnov, A., Holben, B. N., King, M. D., Kaufman, Y. J., Eck, T. F., and Slutsker, I.: Accuracy assessments of aerosol optical properties retrieved from Aerosol Robotic Network (AERONET) Sun and sky radiance measurements, *J. Geophys. Res.*, 105, 9791–9806, 2000.
- Dubovik, O., Sinyuk, A., Lapyonok, T., Holben, B. N., Mishchenko, M., Yang, P., Eck, T. F., Volten, H., Muñoz, O., Veihelmann, B., van der Zande, W. J., Leon, J.-F., Sorokin, M., and Slutsker, I.: Application of spheroid models to account for aerosol particle nonsphericity in remote sensing of desert dust, *J. Geophys. Res.*, 111, D11208, doi:10.1029/2005JD006619, 2006.
- Eck, T. F., Holben, B. N., Slutsker, I., and Setzer, A.: Measurements of irradiance attenuation and estimation of aerosol single scattering albedo for biomass burning aerosols in Amazonia, *J. Geophys. Res.*, 103, 31865–31878, 1998.
- Eck, T. F., Holben, B. N., Reid, J. S., Dubovik, O., Smirnov, A., O'Neill, N. T., Slutsker, I., and Kinne, S.: Wavelength dependence of the optical depth of biomass burning, urban, and desert dust aerosols, *J. Geophys. Res.*, 104, 31333–31349, 1999.
- Eck, T. F., Holben, B. N., Reid, J. S., O'Neill, N. T., Schafer, J. S., Dubovik, O., Smirnov, A., Yamasoe, M. A., and Artaxo, P.: High aerosol optical depth biomass burning events: A com-

[Title Page](#)[Abstract](#)[Introduction](#)[Conclusions](#)[References](#)[Tables](#)[Figures](#)[◀](#)[▶](#)[◀](#)[▶](#)[Back](#)[Close](#)[Full Screen / Esc](#)[Printer-friendly Version](#)[Interactive Discussion](#)

parison of optical properties for different source regions, *Geophys. Res. Lett.*, 30, 2035, doi:10.1029/2003GL017861, 2003.

ESA: Reports for Mission Selection, The Six Candidate Earth Explorer Missions, EarthCARE – Earth Clouds, Aerosols and Radiation Explorer, ESA-SP-1279(1), 2004.

5 Freudenthaler, V., Esselborn, M., Wiegner, M., Heese, B., Tesche, M., Ansmann, A., Müller, D., Althausen, D., Wirth, M., Fix, A., Ehret, G., Knippertz, P., Toledano, C., Gasteiger, J., Garhammer, M., and Seefeldner, M.: Depolarization ratio profiling at several wavelengths in pure Saharan dust during SAMUM 2006, *Tellus B*, 61, 165–179, doi:10.3402/tellusb.v61i1.16821, 2009.

10 Freudenthaler, V., Gross, S., Engelmann, R., Mattis, I., Wandinger, U., Pappalardo, G., Amodeo, A., Giunta, A., D'Amico, G., Chaikovsky, A., Osipenko, F., Slesar, A., Nicolae, D., Belegante, L., Talianu, C., Serikov, I., Linne, H., Jansen, F., Wilson, K., de Graaf, M., Apituley, A., Trickl, T., Giehl, H., and Adam, M.: EARLI09 – direct intercomparison of eleven EARLINET lidar systems, in: Proceedings of the 25th International Laser Radar Conference, St. Petersburg, Russia, 5–9 July, 891–894, 2010.

15 Groß, S., Tesche, M., Freudenthaler, V., Toledano, C., Wiegner, M., Ansmann, A., Althausen, D., and Seefeldner, M.: Characterization of Saharan dust, marine aerosols and a mixture of biomass burning aerosols and dust by means of multiwavelength depolarization and Raman measurements during SAMUM-2, *Tellus B*, 63, 706–724, doi:10.1111/j.1600-0889.2011.00556.x, 2011a.

20 Groß, S., Freudenthaler, V., Wiegner, M., Gasteiger, J., Geiß, A., and Schnell, F.: Dual-wavelength linear depolarization ratio of volcanic aerosols: Lidar measurements of the Eyjafjallajökull plume over Maisach, Germany, *Atmos. Environ.*, 48, 85–96, doi:10.1016/j.atmosenv.2011.06.017, 2011b.

25 Hasekamp, O., Litvinov, P., and Butz, A.: Aerosol properties over the ocean from PARASOL multi-angle photopolarimetric measurements, *J. Geophys. Res.*, 116, D14204, doi:10.1029/2010JD015469, 2011.

Hess, M., Köpke, P., and Schult, I., Optical properties of aerosols and clouds: the software package OPAC, *Bull. Am. Meteorol. Soc.* 79, 831–844, 1998.

30 Holben, B. N., Eck, T. F., Slutsker, I., Tanre, D., Buis, J. P., Setzer, A., Vermote, E., Reagan, J. A., Kaufman, Y. J., and Nakajima, T.: AERONET – A federated instrument network and data archive for aerosol characterization, *Remote Sens. Environ.*, 66, 1–16, 1998.

Title Page

Abstract

Introduction

Conclusions

References

Tables

Figures

◀

▶

◀

▶

Back

Close

Full Screen / Esc

Printer-friendly Version

Interactive Discussion



LIVAS: a 3-D multi-wavelength aerosol/cloud climatology

V. Amiridis et al.

- Holben, B. N., Tanré, D., Smirnov, A., Eck, T. F., Slutsker, I., Abuhaman, N., Newcomb, W. W., Schafer, J. S., Chatenet, B., Lavenue, F., Kaufman, Y. J., Vande Castle, J., Setzer, A., Markham, B., Clark, D., Frouin, R., Halthore, R., Karneli, A., O'Neill, N. T., Pietras, C., Pinker, R. T., Voss, K., and Zibordi, G.: An emerging ground-based aerosol climatology: Aerosol optical depth from AERONET, *J. Geophys. Res.-Atmos.*, 106, 12067–12097, doi:10.1029/2001JD900014, 2001.
- Holler, R., Ito, K., Tohno, S., and Kasahara, M.: Wavelengthdependent aerosol single-scattering albedo: Measurements and model calculations for a coastal site near the Sea of Japan during ACE-Asia, *J. Geophys. Res.*, 108, 8648, doi:10.1029/2002JD003250, 2003.
- Illingworth, A., Barker, H., Beljaars, A., Ceccaldi, M., Chepfer, H., Colec, J., Delanoe, J., Domenech, C., Donovan, D., Fukuda, S., Hirakata, M., Hogan, R., Huenerbein, A., Kollias, P., Kubota, T., Nakajima, T., Nakajima, T., Nishizawa, T., Ohno, Y., Okamoto, H., Oki, R., Sato, K., Satoh, M., Shephard, M., Wandinger, U., Wehr, T., and Zadelhoff, G.-J.: The EARTHCARE satellite: the next step forward in global measurements of clouds, aerosols, precipitation and radiation, *BAMS-D-12-00227*, doi:10.1175/BAMS-D-12-00227.1, (in print), 2014.
- Jung, J., Kim, Y. J., Lee, K. Y., -Cayetano, M. G., Batmunkh, T., Koo, J.-H., and Kim, J.: Spectral optical properties of long-range transport Asian dust and pollution aerosols over Northeast Asia in 2007 and 2008, *Atmos. Chem. Phys.*, 10, 5391–5408, doi:10.5194/acp-10-5391-2010, 2010.
- Kanitz, T., Ansmann, A., Foth, A., Seifert, P., Wandinger, U., Engelmann, R., Baars, H., Althausen, D., Casiccia, C., and Zamorano, F.: Surface matters: limitations of CALIPSO V3 aerosol typing in coastal regions, *Atmos. Meas. Tech.*, 7, 2061–2072, doi:10.5194/amt-7-2061-2014, 2014.
- Kim, S.-W., Yoon, S.-C., Kim, J., and Kim, S.-Y.: Seasonal and monthly variations of columnar aerosol optical properties over East Asia determined from multi-year MODIS, LIDAR, and AERONET Sun/sky radiometer measurements, *Atmos. Environ.*, 41, 1634–1651, 2007.
- Liu, Z., Vaughan, M., Winker, D., Kittaka, C., Getzewich, B., Kuehn, R., Omar, A., Powell, K., Trepte, C., and Hostetler, C.: The CALIPSO Lidar Cloud and Aerosol Discrimination: Version 2 Algorithm and Initial Assessment of Performance, *J. Atmos. Oceanic Technol.*, 26, 1198–1213, doi:10.1175/2009jtech1229.1, 2009.
- Mamouri, R. E., Ansmann, A., Nisantzi, A., Kokkalis, P., Schwarz, A., and Hadjimitsis, D.: Low Arabian dust extinction-to-backscatter ratio, *Geophys. Res. Lett.*, 40, 4762–4766, doi:10.1002/grl.50898, 2013.

[Title Page](#)[Abstract](#)[Introduction](#)[Conclusions](#)[References](#)[Tables](#)[Figures](#)[Back](#)[Close](#)[Full Screen / Esc](#)[Printer-friendly Version](#)[Interactive Discussion](#)

- Marseille, G. J., Houchi, K., de Kloe, J., and Stoffelen, A.: The definition of an atmospheric database for Aeolus, *Atmos. Meas. Tech.*, 4, 67–88, doi:10.5194/amt-4-67-2011, 2011.
- Matthias V., Freudenthaler, V., Amodeo, A., Balin, I., Balis, D., Bösenberg, J., Chaikovsky, A., Chourdakis, G., Comeron, A., Delaval, A., De Tomasi, F., Eixmann, R., Hågård, A., Komguem, L., Kreipl, S., Matthey, R., Rizi, V., Rodrigues, J. A., Wandinger, U., and Wang, X.: Aerosol lidar inter-comparison in the framework of the EARLINET project. 1 Instruments, *Appl. Opt.*, 43, 961–976, 2004.
- McConnell, C. L., Highwood, E. J., Coe, H., Formenti, P., Anderson, B., Osborne, S., Nava, S., Desboeufs, K., Chen, G., and Harrison, M. A. J.: Seasonal variations of the physical and optical characteristics of Saharan dust: Results from the Dust Outflow and Deposition to the Ocean (DODO) experiment, *J. Geophys. Res.*, 113, D14S05, doi:10.1029/2007JD009606, 2008.
- Mie, G.: Beiträge zur Optik trüber Medien, speziell kolloidaler Metallösungen, *Ann. Phys.*, 25, 377–445, 1908.
- Mishchenko, M. I., Travis, L. D., and Lacis, A. A.: Scattering, Absorption, and Emission of Light by Small Particles, Cambridge Univ. Press, New York, available at: <http://www.giss.nasa.gov/~crmmim/books.html>, last access: 20 January 2015, 2002.
- Mueller, D., Ansmann, A., Mattis, I., Tesche, M., Wandinger, U., Althausen, D., and Pisani, G.: Aerosol-type-dependent lidar ratios observed with Raman lidar, *J. Geophys. Res.*, 112, D16202, doi:10.1029/2006JD008292, 2007.
- Müller, T., Schladitz, A., Massling, A., Kaaden, N., Wiedensohler, A., and Kandler, K.: Spectral absorption coefficients and imaginary parts of refractive indices of Saharan dust during SAMUM-1, *Tellus*, 61B, 79–95, 2011.
- Omar, A. H., Won, J.-G., Winker, D. M., Yoon, S.-C., Dubovik, O., and McCormick, M. P.: Development of global aerosol models using cluster analysis of Aerosol Robotic Network (AERONET) measurements, *J. Geophys. Res.*, 110, 1984–2012, doi:10.1029/2004JD004874, 2005.
- Omar, A. H., Winker, D. M., Kittaka, C., Vaughan, M. A., Liu, Z. Y., Hu, Y. X., Trepte, C. R., Rogers, R. R., Ferrare, R. A., Lee, K. P., Kuehn, R. E., and Hostetler, C. A.: The CALIPSO automated aerosol classification and lidar ratio selection algorithm, *J. Atmos. Ocean. Tech.*, 26, 1994–2014, doi:10.1175/2009jtecha1231.1, 2009.

LIVAS: a 3-D multi-wavelength aerosol/cloud climatology

V. Amiridis et al.

[Title Page](#)

[Abstract](#)

[Introduction](#)

[Conclusions](#)

[References](#)

[Tables](#)

[Figures](#)

◀

▶

◀

▶

[Back](#)

[Close](#)

[Full Screen / Esc](#)

[Printer-friendly Version](#)

[Interactive Discussion](#)



LIVAS: a 3-D multi-wavelength aerosol/cloud climatology

V. Amiridis et al.

[Title Page](#)

[Abstract](#)

[Introduction](#)

[Conclusions](#)

[References](#)

[Tables](#)

[Figures](#)



[Full Screen / Esc](#)

[Printer-friendly Version](#)

[Interactive Discussion](#)



LIVAS: a 3-D multi-wavelength aerosol/cloud climatology

V. Amiridis et al.

[Title Page](#)

[Abstract](#)

[Introduction](#)

[Conclusions](#)

[References](#)

[Tables](#)

[Figures](#)

◀

▶

◀
Back

▶
Close

[Full Screen / Esc](#)

[Printer-friendly Version](#)

[Interactive Discussion](#)



Smirnov, A., Holben, B. N., Kaufman, Y. J., Dubovik, O., Eck, T. F., Slutsker, I., Pietras, C., and Halthore, R. N.: Optical properties of atmospheric aerosol in maritime environments, *J. Atmos. Sci.*, 59, 501–523, 2002.

5 Stoffelen, A., Pailleux, J., Källén, E., Vaughan, J.M., Isaksen, L., Flamant, P., Wergen, W., Andersson, E., Schyberg, H., Culoma, A., Meynart, R., Endemann, M., and Ingmann, P.: The Atmospheric Dynamics Mission for Global Wind Field Measurements, *Bull. Am. Meteorol. Soc.*, 86, 73–87, 2005.

10 Tesche, M., Wandinger, U., Ansmann, A., Althausen, D., Müller, D., and Omar, A. H.: Ground-based validation of CALIPSO observations of dust and smoke in the Cape Verde region, *J. Geophys. Res.*, 118, 1–14, doi:10.1002/jgrd.50248, 2013.

15 The EARLINET publishing group 2000–2010: Adam, M., Alados-Arboledas, L., Althausen, D., Amiridis, V., Amodeo, A., Ansmann, A., Apituley, A., Arshinov, Y., Balis, D., Belegante, L., Bobrovnikov, S., Boselli, A., Bravo-Aranda, J. A., Bösenberg, J., Carstea, E., Chaikovsky, A., Comerón, A., D'Amico, G., Daou, D., Dreischuh, T., Engelmann, R., Finger, F., Freudenthaler, V., García-Vizcaino, D., García, A. J. F., Geiß, A., Giannakaki, E., Giehl, H., Giunta, A., de Graaf, M., Granados-Muñoz, M. J., Grein, M., Grigorov, I., Groß, S., Gruening, C., Guerrero-Rascado, J. L., Haeflalin, M., Hayek, T., Iarlori, M., Kanitz, T., Kokkalis, P., Linné, H., Madonna, F., Mamouriat, R.-E., Matthias, V., Mattis, I., Menéndez, F. M., Mitev, V., Mona, L., Morille, Y., Muñoz, C., Müller, A., Müller, D., Navas-Guzmán, F., Nemuc, A., Nicolae, D., Pandolfi, M., Papayannis, A., Pappalardo, G., Pelon, J., Perrone, M. R., Pietruczuk, A., Pisani, G., Potma, C., Preißler, J., Pujadas, M., Putaud, J., Radu, C., Ravetta, F., Reigert, A., Rizi, V., Rocadenbosch, F., Rodríguez, A., Sauvage, L., Schmidt, J., Schnell, F., Schwarz, A., Seifert, P., Serikov, I., Sicard, M., Silva, A. M., Simeonov, V., Siomos, N., Sirci, T., Spinelli, N., Stoyanov, D., Talianu, C., Tesche, M., De Tomasi, F., Trickl, T., Vaughan, G., Volten, H., Wagner, F., Wandinger, U., Wang, X., Wiegner, M., and Wilson, K. M.: EARLINET all observations (2000–2010), World Data Center for Climate (WDCC), available at: http://cera-www.dkrz.de/WDCC/ui/Compact.jsp?acronym=EN_all_measurements_2000-2010, 2014a.

20 The EARLINET publishing group 2000–2010: Adam, M., Alados-Arboledas, L., Althausen, D., Amiridis, V., Amodeo, A., Ansmann, A., Apituley, A., Arshinov, Y., Balis, D., Belegante, L., Bobrovnikov, S., Boselli, A., Bravo-Aranda, J. A., Bösenberg, J., Carstea, E., Chaikovsky, A., Comerón, A., D'Amico, G., Daou, D., Dreischuh, T., Engelmann, R., Finger, F., Freudenthaler, V., García-Vizcaino, D., García, A. J. F., Geiß, A., Giannakaki, E., Giehl, H., Giunta, A., de Graaf, M., Granados-Muñoz, M. J., Grein, M., Grigorov, I., Groß, S., Gruening, C.,

Guerrero-Rascado, J. L., Haeffelin, M., Hayek, T., Iarlori, M., Kanitz, T., Kokkalis, P., Linné, H., Madonna, F., Mamouriat, R.E., Matthias, V., Mattis, I., Menéndez, F. M., Mitev, V., Mona, L., Morille, Y., Muñoz, C., Müller, A., Müller, D., Navas-Guzmán, F., Nemuc, A., Nicolae, D., Pandolfi, M., Papayannis, A., Pappalardo, G., Pelon, J., Perrone, M.R., Pietruczuk, A., Pisani, G., Potma, C., Preißler, J., Pujadas, M., Putaud, J., Radu, C., Ravetta, F., Reigert, A., Rizi, V., Rocadenbosch, F., Rodríguez, A., Sauvage, L., Schmidt, J., Schnell, F., Schwarz, A., Seifert, P., Serikov, I., Sicard, M., Silva, A. M., Simeonov, V., Siomos, N., Sirch, T., Spinelli, N., Stoyanov, D., Talianu, C., Tesche, M., De Tomasi, F., Trickl, T., Vaughan, G., Volten, H., Wagner, F., Wandinger, U., Wang, X., Wiegner, M., and Wilson, K. M.: EARLINET climatology (2000–2010), World Data Center for Climate (WDCC), available at: http://dx.doi.org/10.1594/Wdcc/EN_Climatology_2000-2010, 2014b.

The EARLINET publishing group 2000–2010: Adam, M., Alados-Arboledas, L., Althausen, D., Amiridis, V., Amodeo, A., Ansmann, A., Apituley, A., Arshinov, Y., Balis, D., Belegante, L., Bobrovnikov, S., Boselli, A., Bravo-Aranda, J. A., Bösenberg, J., Carstea, E., Chaikovsky, A., Comerón, A., D'Amico, G., Daou, D., Dreischuh, T., Engelmann, R., Finger, F., Freudenthaler, V., García-Vizcaino, D., García, A. J. F., Geiß, A., Giannakaki, E., Giehl, H., Giunta, A., de Graaf, M., Granados-Muñoz, M. J., Grein, M., Grigorov, I., Groß, S., Gruening, C., Guerrero-Rascado, J. L., Haeffelin, M., Hayek, T., Iarlori, M., Kanitz, T., Kokkalis, P., Linné, H., Madonna, F., Mamouriat, R.-E., Matthias, V., Mattis, I., Menéndez, F. M., Mitev, V., Mona, L., Morille, Y., Muñoz, C., Müller, A., Müller, D., Navas-Guzmán, F., Nemuc, A., Nicolae, D., Pandolfi, M., Papayannis, A., Pappalardo, G., Pelon, J., Perrone, M. R., Pietruczuk, A., Pisani, G., Potma, C., Preißler, J., Pujadas, M., Putaud, J., Radu, C., Ravetta, F., Reigert, A., Rizi, V., Rocadenbosch, F., Rodríguez, A., Sauvage, L., Schmidt, J., Schnell, F., Schwarz, A., Seifert, P., Serikov, I., Sicard, M., Silva, A. M., Simeonov, V., Siomos, N., Sirch, T., Spinelli, N., Stoyanov, D., Talianu, C., Tesche, M., De Tomasi, F., Trickl, T., Vaughan, G., Volten, H., Wagner, F., Wandinger, U., Wang, X., Wiegner, M., and Wilson, K. M.: EARLINET correlative observations for CALIPSO (2006–2010), World Data Center for Climate (WDCC), available at: http://dx.doi.org/10.1594/Wdcc/EN_Calipso_2006-2010, 2014c.

The EARLINET publishing group 2000–2010, Adam, M., Alados-Arboledas, L., Althausen, D., Amiridis, V., Amodeo, A., Ansmann, A., Apituley, A., Arshinov, Y., Balis, D., Belegante, L., Bobrovnikov, S., Boselli, A., Bravo-Aranda, J. A., Bösenberg, J., Carstea, E., Chaikovsky, A., Comerón, A., D'Amico, G., Daou, D., Dreischuh, T., Engelmann, R., Finger, F., Freudenthaler, V., García-Vizcaino, D., García, A. J. F., Geiß, A., Giannakaki, E., Giehl, H., Giunta,

LIVAS: a 3-D multi-wavelength aerosol/cloud climatology

V. Amiridis et al.

[Title Page](#)

[Abstract](#)

[Introduction](#)

[Conclusions](#)

[References](#)

[Tables](#)

[Figures](#)



[Full Screen / Esc](#)

[Printer-friendly Version](#)

[Interactive Discussion](#)



A., de Graaf, M., Granados-Muñoz, M. J., Grein, M., Grigorov, I., Groß, S., Gruening, C., Guerrero-Rascado, J. L., Haeffelin, M., Hayek, T., Iarlori, M., Kanitz, T., Kokkalis, P., Linné, H., Madonna, F., Mamouri, R.-E., Matthias, V., Mattis, I., Menéndez, F. M., Mitev, V., Mona, L., Morille, Y., Muñoz, C., Müller, A., Müller, D., Navas-Guzmán, F., Nemuc, A., Nicolae, D., Pandolfi, M., Papayannis, A., Pappalardo, G., Pelon, J., Perrone, M. R., Pietruczuk, A., Pisani, G., Potma, C., Preißler, J., Pujadas, M., Putaud, J., Radu, C., Ravetta, F., Reigert, A., Rizi, V., Rocadenbosch, F., Rodríguez, A., Sauvage, L., Schmidt, J., Schnell, F., Schwarz, A., Seifert, P., Serikov, I., Sicard, M., Silva, A. M., Simeonov, V., Siomos, N., Sirc, T., Spinelli, N., Stoyanov, D., Talianu, C., Tesche, M., De Tomasi, F., Trickl, T., Vaughan, G., Volten, H., Wagner, F., Wandinger, U., Wang, X., Wiegner, M., and Wilson, K. M.: EARLINET observations related to volcanic eruptions (2000–2010), World Data Center for Climate (WDCC), available at: http://dx.doi.org/10.1594/WDCC/EN_VolcanicEruption_2000-2010, 2014d.

The EARLINET publishing group 2000–2010: Adam, M., Alados-Arboledas, L., Althausen, D., Amiridis, V., Amodeo, A., Ansmann, A., Apituley, A., Arshinov, Y., Balis, D., Belegante, L., Bobrovnikov, S., Boselli, A., Bravo-Aranda, J. A., Bösenberg, J., Carstea, E., Chaikovsky, A., Comerón, A., D'Amico, G., Daou, D., Dreischuh, T., Engelmann, R., Finger, F., Freudenthaler, V., García-Vizcaino, D., García, A. J. F., Geiß, A., Giannakaki, E., Giehl, H., Giunta, A., de Graaf, M., Granados-Muñoz, M. J., Grein, M., Grigorov, I., Groß, S., Gruening, C., Guerrero-Rascado, J. L., Haeffelin, M., Hayek, T., Iarlori, M., Kanitz, T., Kokkalis, P., Linné, H., Madonna, F., Mamouri, R.-E., Matthias, V., Mattis, I., Menéndez, F. M., Mitev, V., Mona, L., Morille, Y., Muñoz, C., Müller, A., Müller, D., Navas-Guzmán, F., Nemuc, A., Nicolae, D., Pandolfi, M., Papayannis, A., Pappalardo, G., Pelon, J., Perrone, M. R., Pietruczuk, A., Pisani, G., Potma, C., Preißler, J., Pujadas, M., Putaud, J., Radu, C., Ravetta, F., Reigert, A., Rizi, V., Rocadenbosch, F., Rodríguez, A., Sauvage, L., Schmidt, J., Schnell, F., Schwarz, A., Seifert, P., Serikov, I., Sicard, M., Silva, A. M., Simeonov, V., Siomos, N., Sirc, T., Spinelli, N., Stoyanov, D., Talianu, C., Tesche, M., De Tomasi, F., Trickl, T., Vaughan, G., Volten, H., Wagner, F., Wandinger, U., Wang, X., Wiegner, M., and Wilson, K. M.: EARLINET observations related to Saharan Dust events (2000–2010), World Data Center for Climate (WDCC), available at: http://dx.doi.org/10.1594/WDCC/EARLINET_SaharanDust_2000-2010, 2014e.

Toledano, C., Wiegner, M., Gross, S., Freudenthaler, V., Gasteiger, J., Müller, D., Müller, T., Schladitz, A., Weinzierl, B., Torres B., and O'Neill, N. T.: Optical properties of aerosol mixtures derived from sun-sky radiometry during SAMUM-2, Tellus, 63B, 635–648, doi:10.1111/j.1600-0889.2011.00573.x, 2011.

LIVAS: a 3-D multi-wavelength aerosol/cloud climatology

V. Amiridis et al.

[Title Page](#)

[Abstract](#)

[Introduction](#)

[Conclusions](#)

[References](#)

[Tables](#)

[Figures](#)

◀

▶

◀

▶

[Back](#)

[Close](#)

[Full Screen / Esc](#)

[Printer-friendly Version](#)

[Interactive Discussion](#)



- Van de Hulst, H.: Light Scattering by Small Particles, Wiley, New York, 1957.
- Vaughan, M. A., Powell, K. A., Kuehn, R. E., Young, S. A., Winker, D. M., Hostetler, C. A., Hunt, W. H., Liu, Z. Y., McGill, M. J., and Getzewich, B. J.: Fully automated detection of cloud and aerosol layers in the CALIPSO lidar measurements, *J. Atmos. Ocean. Tech.*, 26, 2034–2050, doi:10.1175/2009jtecha1228.1, 2009.
- Volten, H., Munoz, O., Rol, E., de Haan, J. F., Vassen, W., Hovenier, J. W., Muinonen, K., and Nousiainen, T.: Scattering matrices of mineral aerosol particles at 441.6 nm and 632.8 nm, *J. Geophys. Res.*, 106, 17375–17401, 2001.
- Wandinger, U., Ansmann, A., Reichardt, J., and Deshler, T.: Determination of stratospheric aerosol microphysical properties from independent extinction and backscattering measurements with a Raman lidar, *Appl Opt.*, 34, 8315–8329, doi:10.1364/AO.34.008315, 1995.
- Wandinger, U., Tesche, M., Seifert, P., Ansmann, A., Müller, D., and Althausen, D.: Size matters: Influence of multiple scattering on CALIPSO light-extinction profiling in desert dust, *Geophys. Res. Lett.*, 37, L10801, doi:10.1029/2010GL042815, 2010.
- Wandinger, U., Hiebsch, A., Mattis, I., Pappalardo, G., Mona, L., and Madonna, F.: Aerosols and Clouds: Long-term Database from Spaceborne Lidar Measurements, Executive Summary, available at: <http://esamultimedia.esa.int/docs/gsp/C21487ExS.pdf>, last access: 20 January 2015, ESTEC Contract 21487/08/NL/HE, 2011.
- Weinzierl, B., Petzold, A., Esselborn, M., Wirth, M., Rasp, K., Kandler, K., Schütz, L., Koepke P., and Fiebig, M.: Airborne measurements of dust layer properties, particle size distribution and mixing state of Saharan dust during SAMUM 2006, *Tellus* 61B, 96–117, doi:10.1111/j.1600-0889.2008.00392.x, 2009.
- Winker, D. M., Vaughan, M. A., Omar, A., Hu, Y., Powell, K. A., Liu, Z., Hunt, W. H., and Young, S. A.: Overview of the CALIPSO mission and CALIOP data processing algorithms, *J. Atmos. Ocean. Tech.*, 26, 2310–2323, doi:10.1175/2009JTECHA1281.1, 2009.
- Winker, D. M., Tackett, J. L., Getzewich, B. J., Liu, Z., Vaughan, M. A., and Rogers, R. R.: The global 3-D distribution of tropospheric aerosols as characterized by CALIOP, *Atmos. Chem. Phys.*, 13, 3345–3361, doi:10.5194/acp-13-3345-2013, 2013.
- Yang, P. and Liou, K. N.: Geometric-optics-integral-equation method for light scattering by non-spherical ice crystals, *Appl. Opt.*, 35, 6568–6584, 1996.
- Young, S. A. and Vaughan, M. A.: The retrieval of profiles of particulate extinction from cloud-aerosol lidar infrared pathfinder satellite observations (CALIPSO) data: Algorithm description, *J. Atmos. Ocean. Tech.*, 26, 1105–1119, doi:10.1175/2008JTECHA1221.1, 2009.

[Title Page](#)[Abstract](#)[Introduction](#)[Conclusions](#)[References](#)[Tables](#)[Figures](#)[◀](#)[▶](#)[◀](#)[▶](#)[Back](#)[Close](#)[Full Screen / Esc](#)[Printer-friendly Version](#)[Interactive Discussion](#)

Title Page	
Abstract	Introduction
Conclusions	References
Tables	Figures
◀	▶
◀	▶
Back	Close
Full Screen / Esc	

[Printer-friendly Version](#)[Interactive Discussion](#)

Table 1. The extinction- and backscatter-related Ångström exponents (spectral conversion factors) for each aerosol type used in LIVAS for the conversion from 532 to 355 nm (VIS-UV) and from 532 to 1570 and 2050 nm (VIS-IR). The approaches used for their calculation are also indicated.

LIVAS AEROSOL TYPE	VIS-UV CONVERSION FACTORS				VIS-IR CONVERSION FACTORS			
	approach used	532/355 nm		approach used	532/1570 nm		532/2050 nm	
		bsc	ext		bsc	ext	bsc	ext
Polluted continental Dust	ESA-CALIPSO	1.42	1.24	AERONET-Omar	1.18	1.66	1.32	1.56
	ESA-CALIPSO	0.40	0.55	AERONET-CALIPSO	0.35	0.6	0.43	0.57
Polluted dust	ESA-CALIPSO	0.92	0.71	AERONET-CALIPSO	0.67	1.14	0.71	1.07
Smoke	ESA-CALIPSO	1.46	1.41	AERONET-CALIPSO	0.79	1.42	0.825	1.34
Clean marine	ESA-CALIPSO (bsc) Sayer et al. (2012) (ext)	0.50	0.78	Sayer et al. (2012)	0.74	0.39	0.81	0.38
Clean continental	ESA-CALIPSO (bsc) OPAC (ext)	1.20	1.31	OPAC	1.15	1.28	1.64	1.27
Stratospheric	ESA-CALIPSO (bsc)	0.98	0.48	Deshler et al., (1993) Wandinger et al. (1995)	1.36	1.33	1.38	1.49
	Deshler et al. (1993), Wandinger et al. (1995) (ext)							

LIVAS: a 3-D multi-wavelength aerosol/cloud climatology

V. Amiridis et al.

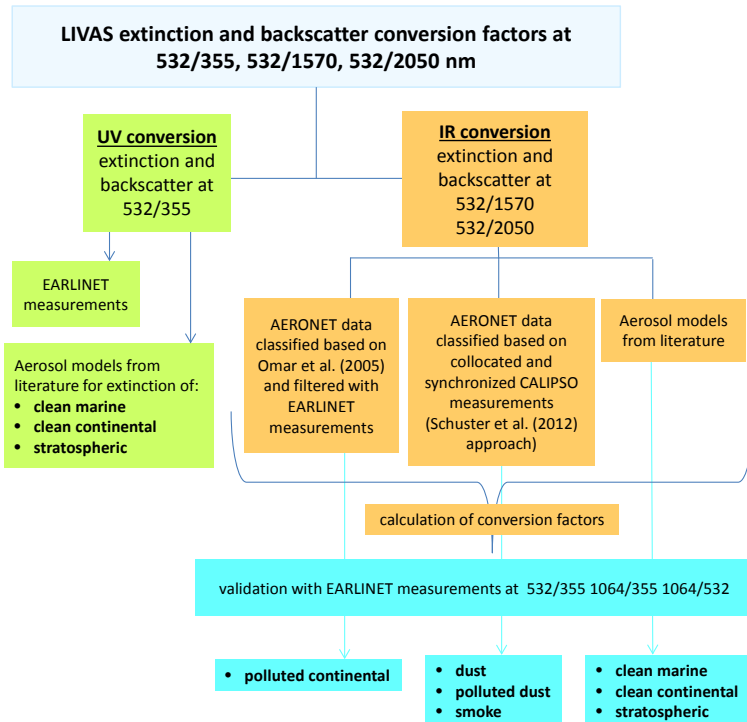


Figure 1. Schematic diagram describing the methodological steps followed for the derivation of LIVAS extinction and backscatter-related conversion factors in the UV and IR.

LIVAS: a 3-D multi-wavelength aerosol/cloud climatology

V. Amiridis et al.

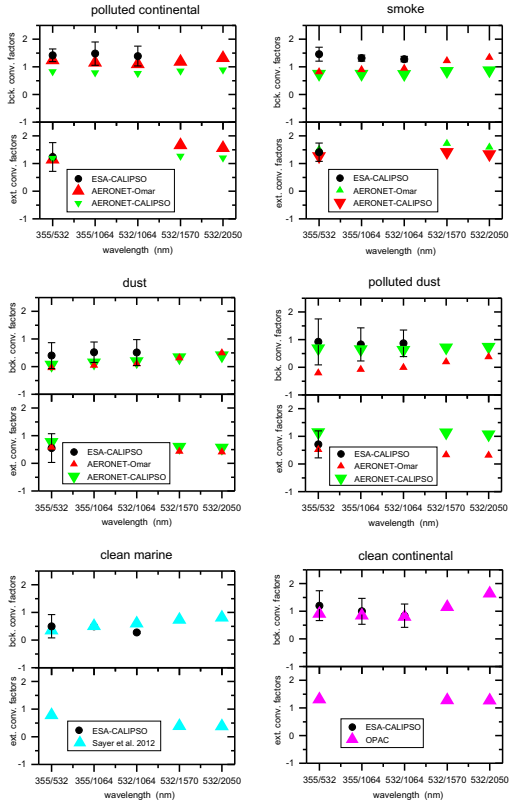


Figure 2. Backscatter (upper) and extinction-related (bottom) VIS-IR conversion factors, calculated with different approaches (i.e. “AERONET-Omar” (red triangles), “AERONET-CALIPSO” (green triangles), “Sayer et al., (2012)” (cyan triangles), “OPAC” (pink triangles)) and validated against the ESA-CALIPSO conversion factors in VIS and UV (black circles). The conversion factors selected and ingested in the LIVAS aerosol model for the VIS-IR conversions, are denoted with symbols of larger size.

LIVAS: a 3-D multi-wavelength aerosol/cloud climatology

V. Amiridis et al.

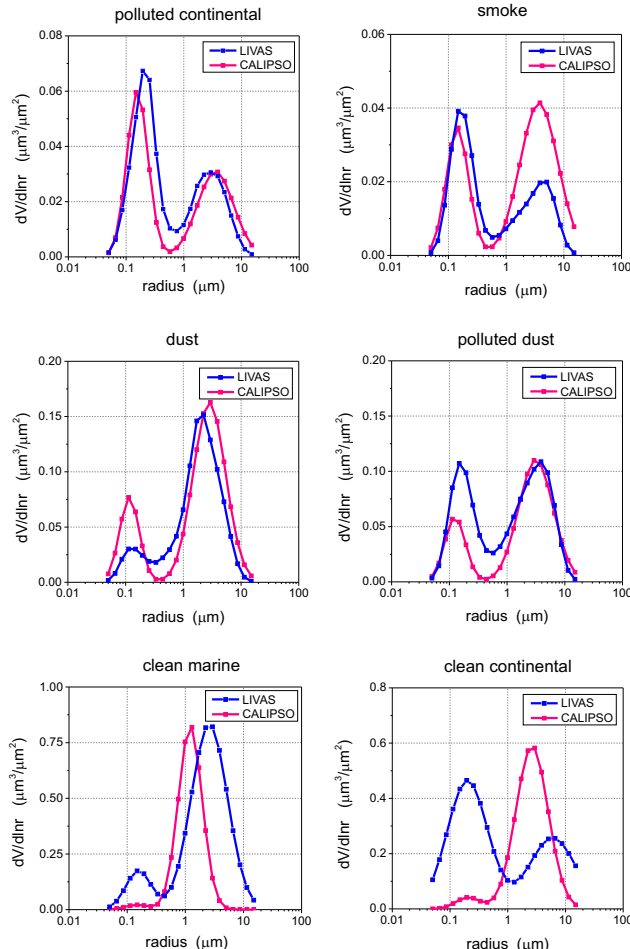


Figure 3. Comparison of the mean volume size distributions for each aerosol type in the LIVAS (blue line) and CALIPSO (pink line) aerosol models.

LIVAS: a 3-D multi-wavelength aerosol/cloud climatology

V. Amiridis et al.

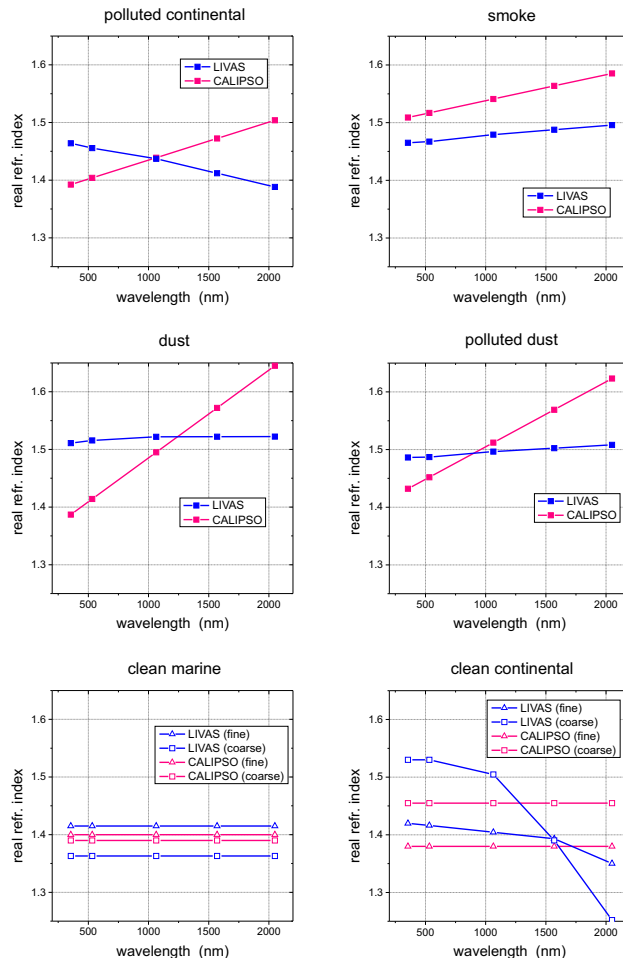


Figure 4. Comparison of the mean real part of the refractive index for each aerosol type in the LIVAS (blue line) and CALIPSO (pink line) aerosol models.

Title Page

Abstract

Introduction

Conclusions

References

Tables

Figures

◀

▶

◀

▶

Back

Close

Full Screen / Esc

Printer-friendly Version

Interactive Discussion

LIVAS: a 3-D multi-wavelength aerosol/cloud climatology

V. Amiridis et al.

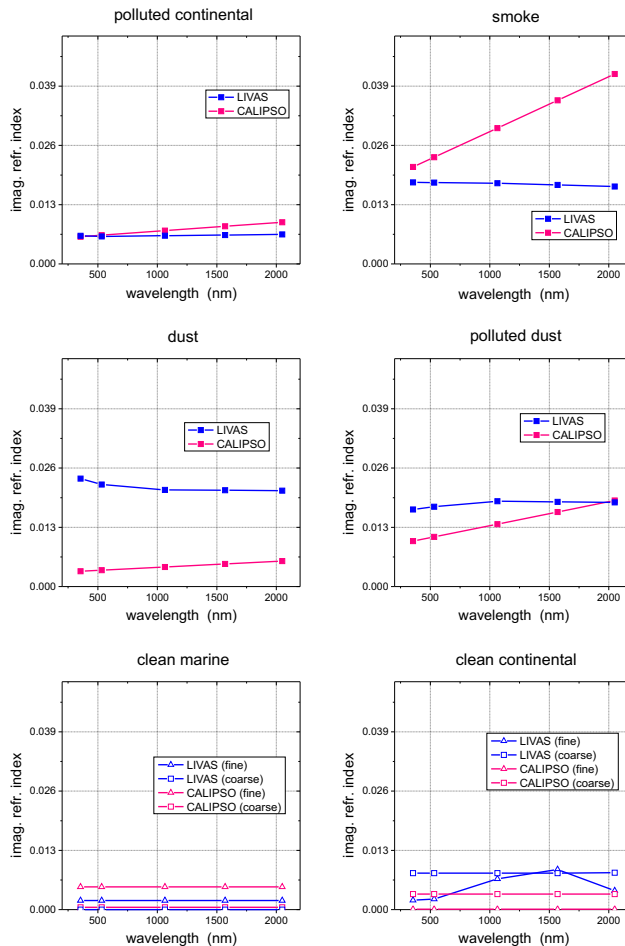


Figure 5. Comparison of the mean imaginary part of the refractive index for each aerosol type in the LIVAS (blue line) and CALIPSO (pink line) aerosol models.

**LIVAS: a 3-D
multi-wavelength
aerosol/cloud
climatology**

V. Amiridis et al.

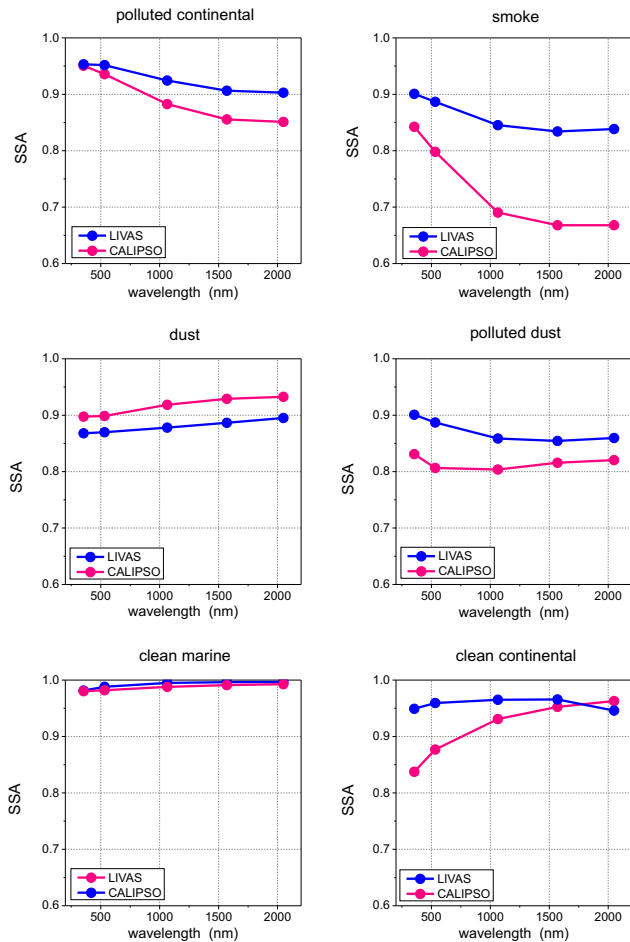


Figure 6. Comparison of the mean spectral SSA for each aerosol type in the LIVAS (blue line) and CALIPSO (pink line) aerosol models.

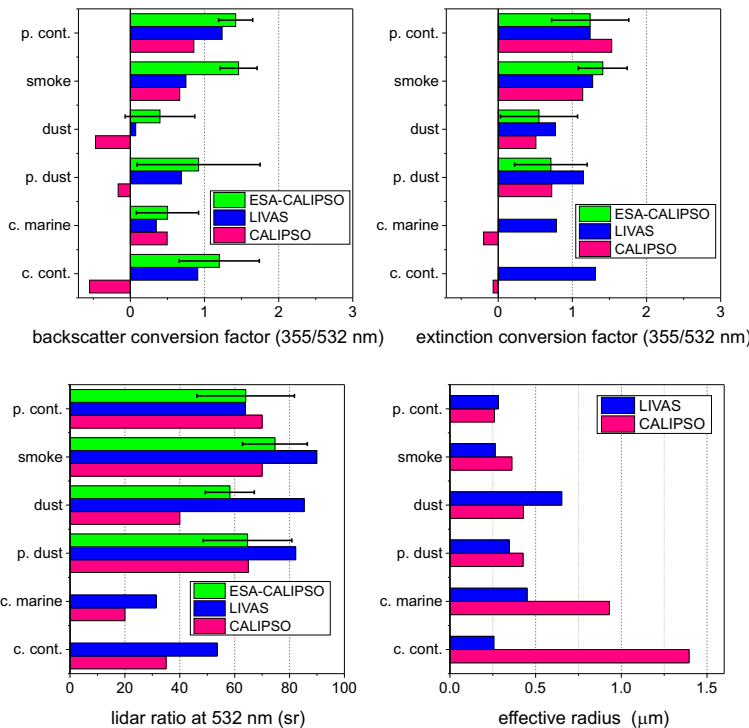


Figure 7. Comparison of the LIVAS and CALIPSO aerosol models with ESA-CALIPSO values for: backscatter-related conversion factor at 355/532 nm (upper-left), extinction-related conversion factor at 355/532 nm (upper-right), lidar ratio at 532 nm (lower-left) and effective radius (lower-right).

**LIVAS: a 3-D
multi-wavelength
aerosol/cloud
climatology**

V. Amiridis et al.

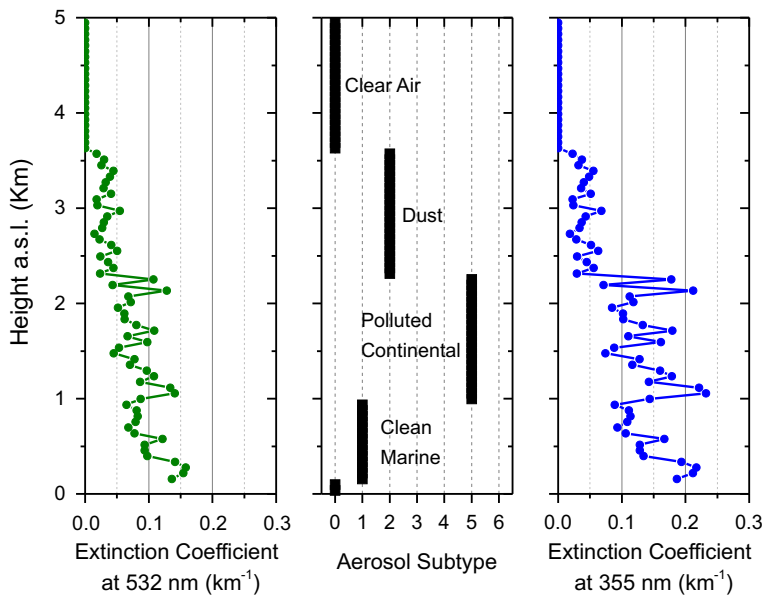


Figure 8. CALIPSO Level 2 extinction coefficient profile at 532 nm (left), aerosol type (center) and converted extinction coefficient at 355 nm (right), based on LIVAS typical conversion factors. The profile example refers to 7 September, 2011, (cell centroid with latitude of 37.5 and longitude of 20.5°).

[Title Page](#)[Abstract](#)[Introduction](#)[Conclusions](#)[References](#)[Tables](#)[Figures](#)[◀](#)[▶](#)[Back](#)[Close](#)[Full Screen / Esc](#)[Printer-friendly Version](#)[Interactive Discussion](#)

Title Page	
Abstract	Introduction
Conclusions	References
Tables	Figures
◀	▶
◀	▶
Back	Close
Full Screen / Esc	
Printer-friendly Version	
Interactive Discussion	

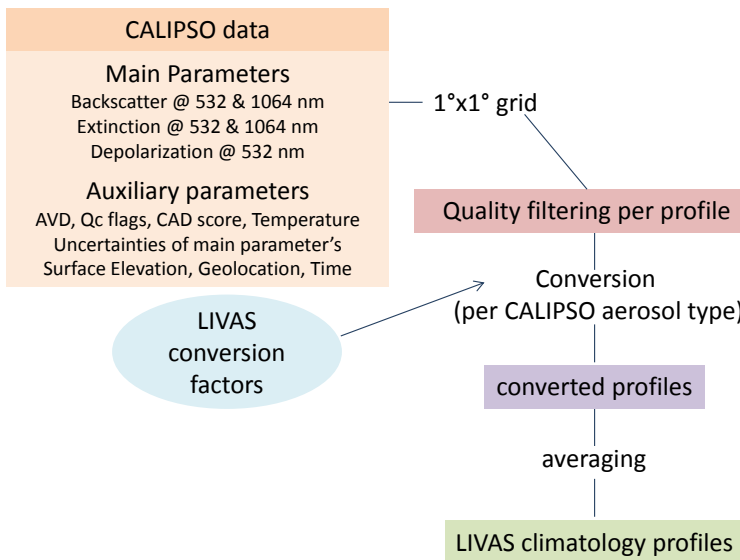


Figure 9. Schematic diagram of LIVAS processing chain.

LIVAS: a 3-D multi-wavelength aerosol/cloud climatology

V. Amiridis et al.

[Title Page](#)

[Abstract](#)

[Introduction](#)

[Conclusions](#)

[References](#)

[Tables](#)

[Figures](#)

◀

▶

[Back](#)

[Close](#)

[Full Screen / Esc](#)

[Printer-friendly Version](#)

[Interactive Discussion](#)

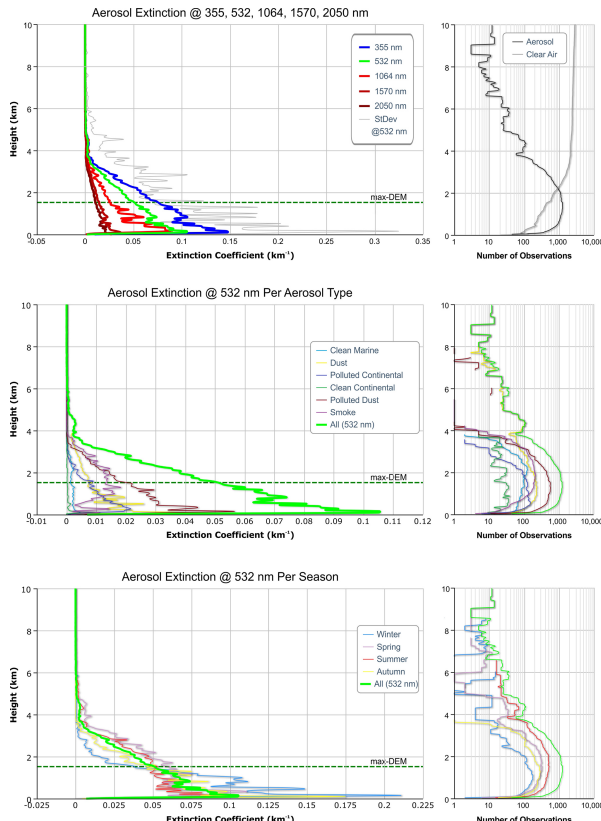


Figure 10. LIVAS aerosol extinction products. Upper panel: vertical distribution of the averaged aerosol extinction coefficient at 355, 532, 1064, 1570, 2050 nm (left), number of observations used in averaging (right). Middle panel: vertical distribution of the averaged aerosol extinction coefficient per aerosol type (left), number of observations used in averaging (right). Lower panel: vertical distribution of the averaged aerosol extinction coefficient per season (left), number of observations used in averaging (right).

LIVAS: a 3-D multi-wavelength aerosol/cloud climatology

V. Amiridis et al.

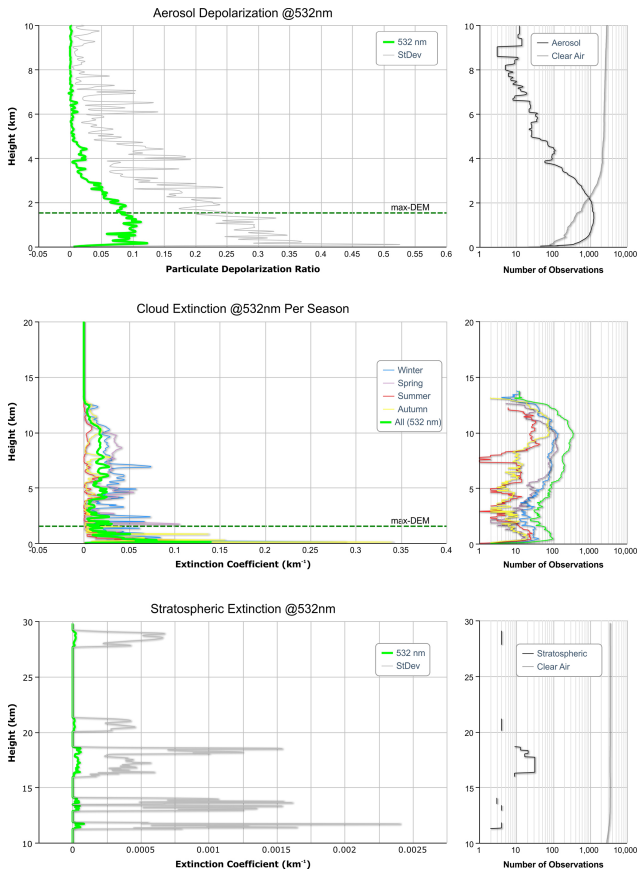


Figure 11. Additional LIVAS products: Upper panel: vertical distribution of the averaged particle depolarization at 532 nm (left), number of observations used in averaging (right). Middle panel: vertical distribution of the averaged cloud extinction coefficient per season (left), number of observations used in averaging (right). Lower panel: vertical distribution of the averaged stratospheric aerosol extinction coefficient (left), number of observations used in averaging (right).

**LIVAS: a 3-D
multi-wavelength
aerosol/cloud
climatology**

V. Amiridis et al.

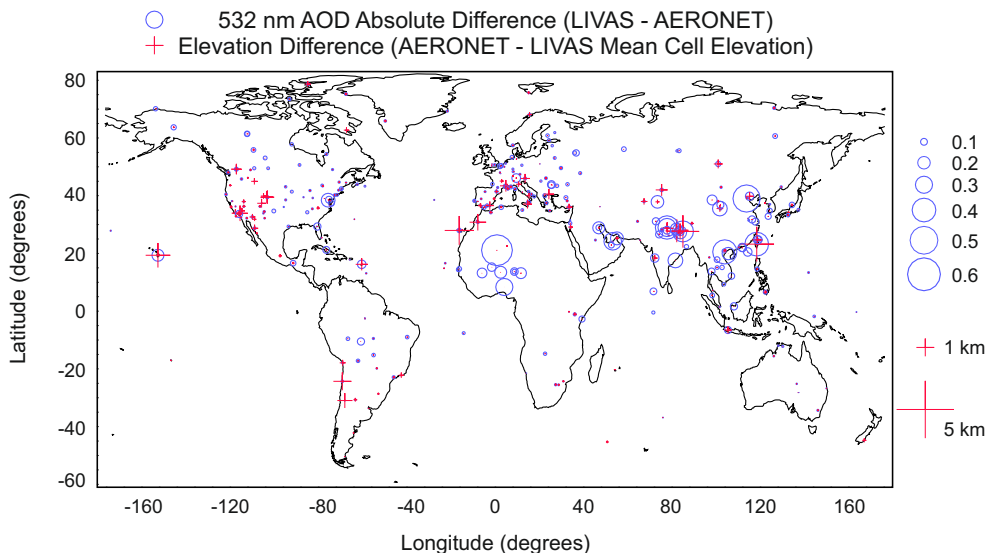


Figure 12. Spatial distribution of the 532 nm AOD absolute differences (absolute value of LIVAS averaged AOD minus AERONET averaged AOD) (blue circles) and of the difference between AERONET site elevation and mean grid cell elevation of CALIPSO overpass (red crosses).

[Title Page](#)[Abstract](#)[Introduction](#)[Conclusions](#)[References](#)[Tables](#)[Figures](#)[◀](#)[▶](#)[◀](#)[▶](#)[Back](#)[Close](#)[Full Screen / Esc](#)[Printer-friendly Version](#)[Interactive Discussion](#)

**LIVAS: a 3-D
multi-wavelength
aerosol/cloud
climatology**

V. Amiridis et al.

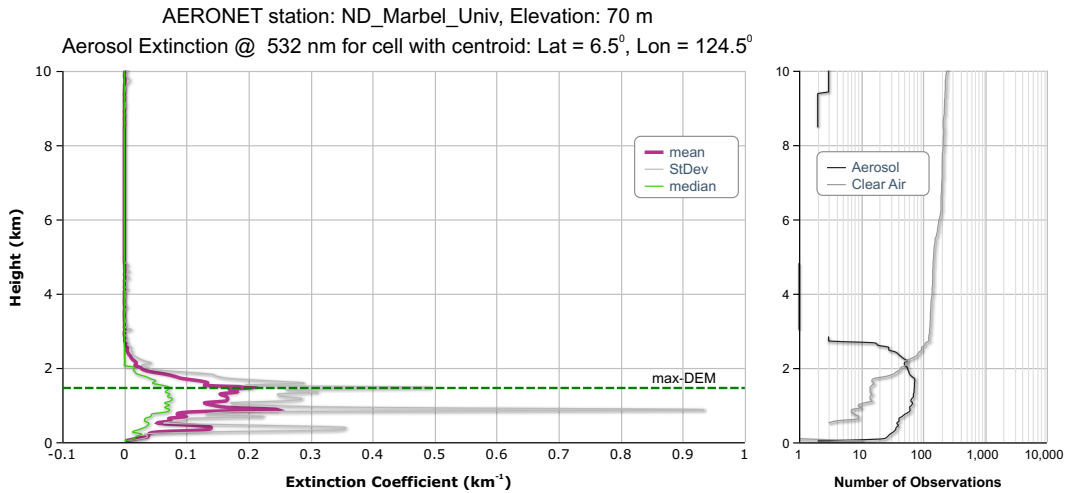


Figure 13. Example of high-slope terrain on CALIPSO overpass for the case of ND_Marbel_Univ AERONET station. Left panel: vertical distribution of the averaged aerosol extinction coefficient. Right panel: number of observations used in averaging.

[Title Page](#)[Abstract](#)[Introduction](#)[Conclusions](#)[References](#)[Tables](#)[Figures](#)[◀](#)[▶](#)[Back](#)[Close](#)[Full Screen / Esc](#)[Printer-friendly Version](#)[Interactive Discussion](#)

**LIVAS: a 3-D
multi-wavelength
aerosol/cloud
climatology**

V. Amiridis et al.

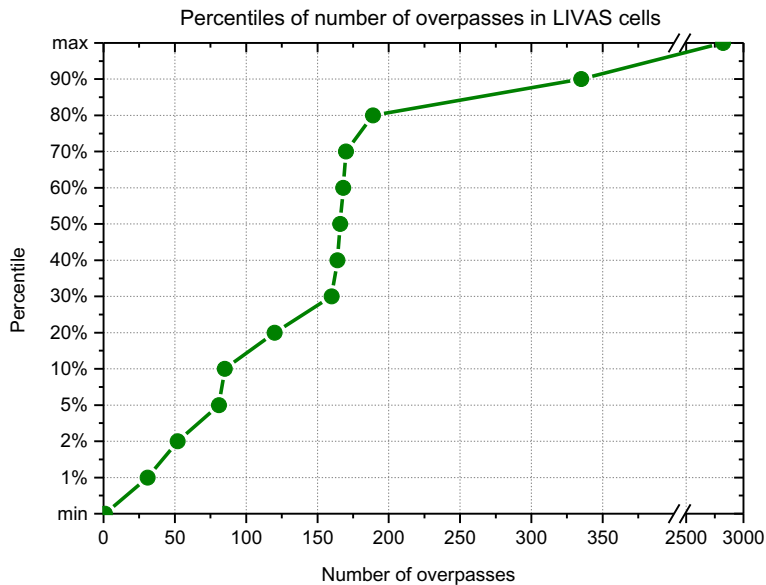


Figure 14. Percentiles of the number of overpasses in LIVAS global grid cells.

**LIVAS: a 3-D
multi-wavelength
aerosol/cloud
climatology**

V. Amiridis et al.

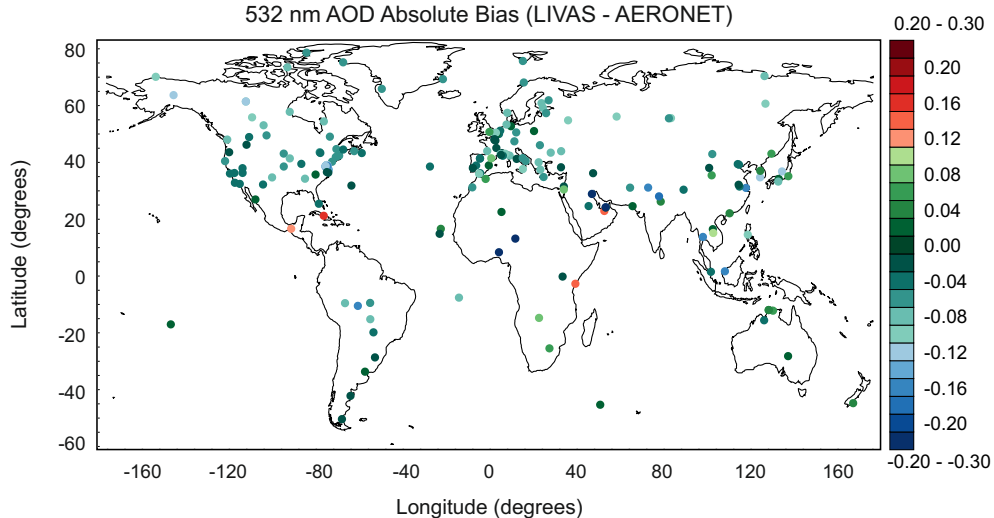


Figure 15. Spatial distribution of the 532 nm AOD absolute biases (LIVAS averaged AOD minus AERONET averaged AOD).

- [Title Page](#)
- [Abstract](#) [Introduction](#)
- [Conclusions](#) [References](#)
- [Tables](#) [Figures](#)
-
-
- [Full Screen / Esc](#)
- [Printer-friendly Version](#)
- [Interactive Discussion](#)

LIVAS: a 3-D multi-wavelength aerosol/cloud climatology

V. Amiridis et al.

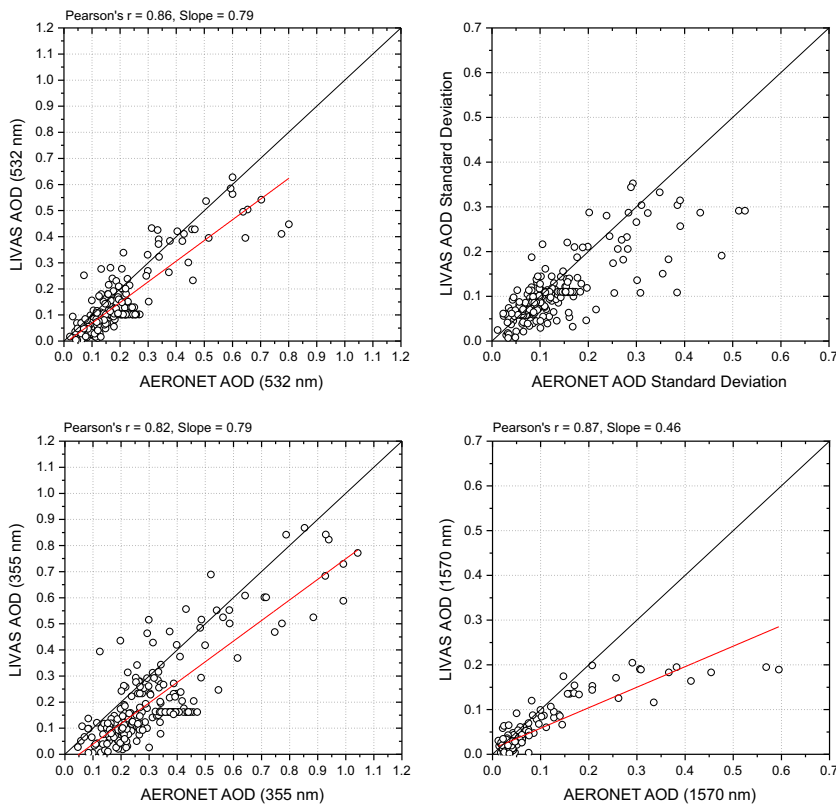


Figure 16. Upper panel: Scatter plot comparison of LIVAS AODs at 532 nm versus collocated AERONET Level 2 product (left) and standard deviation of the LIVAS AODs versus standard deviation of the AERONET AODs at 532 nm (right). Lower panel: Scatter plot comparison of LIVAS AODs at 355 nm versus collocated AERONET Level 2 product (left) and of LIVAS AODs at 1570 nm versus collocated AERONET Level 2 product (right).

- [Title Page](#)
- [Abstract](#) [Introduction](#)
- [Conclusions](#) [References](#)
- [Tables](#) [Figures](#)
- [◀](#) [▶](#)
- [◀](#) [▶](#)
- [Back](#) [Close](#)
- [Full Screen / Esc](#)
- [Printer-friendly Version](#)
- [Interactive Discussion](#)



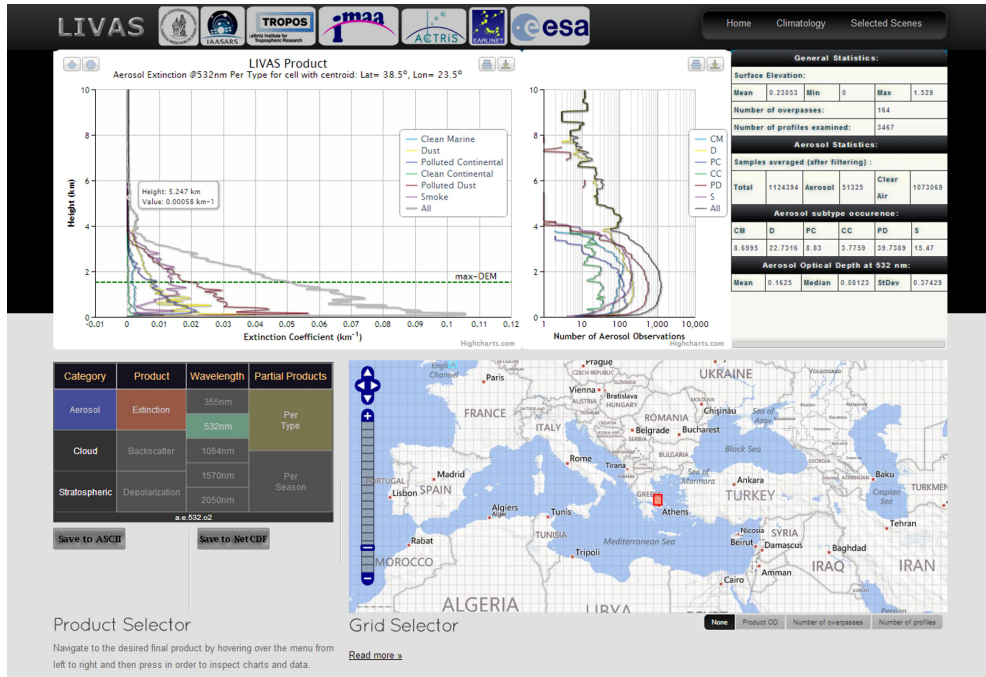


Figure 17. The LIVAS web-portal.

LIVAS: a 3-D multi-wavelength aerosol/cloud climatology

V. Amiridis et al.

[Title Page](#)

[Abstract](#)

[Introduction](#)

[Conclusions](#)

[References](#)

[Tables](#)

[Figures](#)

◀

▶

◀

▶

[Back](#)

[Close](#)

[Full Screen / Esc](#)

[Printer-friendly Version](#)

[Interactive Discussion](#)

LIVAS: a 3-D multi-wavelength aerosol/cloud climatology

V. Amiridis et al.

Figure 18. Global distribution of LIVAS AOD at 532 nm.

Title Page

Abstract

Introduction

Conclusions

References

Tables

Figures

Tables | Figures

Figures

Tables | Figures

Figures

1

▶

◀

▶

Back

Close

Full Screen / Esc

[Printer-friendly Version](#)

Interactive Discussion

